

# Nt-acetylation-independent turnover of SQUALENE EPOXIDASE 1 by Arabidopsis DOA10-like E3 ligases

Etherington, Ross; Bailey, Mark; Boyer, Jean-Baptiste; Armbruster, Laura; Cao, Xulyu; Coates, Juliet; Meinel, Thierry; Wirtz, Markus; Giglione, Carmela; Gibbs, Daniel

DOI:  
[10.1093/plphys/kiad406](https://doi.org/10.1093/plphys/kiad406)

License:  
Creative Commons: Attribution (CC BY)

Document Version  
Peer reviewed version

Citation for published version (Harvard):  
Etherington, R, Bailey, M, Boyer, J-B, Armbruster, L, Cao, X, Coates, J, Meinel, T, Wirtz, M, Giglione, C & Gibbs, D 2023, 'Nt-acetylation-independent turnover of SQUALENE EPOXIDASE 1 by Arabidopsis DOA10-like E3 ligases', *Plant Physiology*. <https://doi.org/10.1093/plphys/kiad406>

[Link to publication on Research at Birmingham portal](#)

## General rights

Unless a licence is specified above, all rights (including copyright and moral rights) in this document are retained by the authors and/or the copyright holders. The express permission of the copyright holder must be obtained for any use of this material other than for purposes permitted by law.

- Users may freely distribute the URL that is used to identify this publication.
- Users may download and/or print one copy of the publication from the University of Birmingham research portal for the purpose of private study or non-commercial research.
- User may use extracts from the document in line with the concept of 'fair dealing' under the Copyright, Designs and Patents Act 1988 (?)
- Users may not further distribute the material nor use it for the purposes of commercial gain.

Where a licence is displayed above, please note the terms and conditions of the licence govern your use of this document.

When citing, please reference the published version.

## Take down policy

While the University of Birmingham exercises care and attention in making items available there are rare occasions when an item has been uploaded in error or has been deemed to be commercially or otherwise sensitive.

If you believe that this is the case for this document, please contact [UBIRA@lists.bham.ac.uk](mailto:UBIRA@lists.bham.ac.uk) providing details and we will remove access to the work immediately and investigate.

1 **Short title:** Nt-acetylation-independent turnover of SQE1

2  
3 **Nt-acetylation-independent turnover of SQUALENE EPOXIDASE 1 by Arabidopsis**  
4 **DOA10-like E3 ligases**

5  
6 Ross D. Etherington<sup>1</sup>, Mark Bailey<sup>1,4</sup>, Jean-Baptiste Boyer<sup>2</sup>, Laura Armbruster<sup>3</sup>, Xulyu Cao<sup>1</sup>,  
7 Juliet C. Coates<sup>1</sup>, Thierry Meinzel<sup>2</sup>, Markus Wirtz<sup>3</sup>, Carmela Giglione<sup>2</sup> and Daniel J. Gibbs<sup>1,\*</sup>

8  
9 <sup>1</sup> School of Biosciences, University of Birmingham, Edgbaston, West Midlands, B15 2TT, UK

10 <sup>2</sup> Université Paris-Saclay, CEA, CNRS, Institute for Integrative Biology of the Cell (I2BC),  
11 91198 Gif-sur-Yvette, France

12 <sup>3</sup> Centre for Organismal Studies Heidelberg, Heidelberg University, Heidelberg, Germany

13 <sup>4</sup> Present address: Plant Sciences Department, Rothamsted Research, Harpenden, AL5  
14 2JQ, UK

15  
16  
17 \*Correspondence: [d.gibbs@bham.ac.uk](mailto:d.gibbs@bham.ac.uk)

18  
19 The author responsible for distribution of materials integral to the findings presented in this  
20 article in accordance with the policy described in the Instructions for Authors  
21 (<https://academic.oup.com/plphys/pages/General-Instructions>) is Daniel Gibbs.

22  
23  
24  
25  
26  
27 **Keywords:**

28 Nt-acetylation, N-terminomics, ubiquitin proteasome system, Ac/N-degron pathway,  
29 proteolysis, Ac/N-recognin, ERAD, sterol biosynthesis

38 **Abstract**

39

40 The Acetylation-dependent (Ac/) N-degron pathway degrades proteins through recognition  
41 of their acetylated N-termini (Nt) by E3-ligases called Ac/N-recognins. To date, specific  
42 Ac/N-recognins have not been defined in plants. Here we used molecular, genetic, and  
43 multi-omics approaches to characterise potential roles for Arabidopsis (*Arabidopsis thaliana*)  
44 DEGRADATION OF ALPHA2 10 (DOA10)-like E3-ligases in the Nt-acetylation-(NTA-)  
45 dependent turnover of proteins at global and protein-specific scales. Arabidopsis has two  
46 ER-localised DOA10-like proteins. *AtDOA10A*, but not the *Brassicaceae*-specific *AtDOA10B*,  
47 can compensate for loss of yeast (*Saccharomyces cerevisiae*) *ScDOA10* function.  
48 Transcriptome and Nt-acetylome profiling of an *Atdoa10a/b* RNAi mutant revealed no  
49 obvious differences in the global NTA profile compared to wildtype, suggesting that  
50 *AtDOA10s* do not regulate the bulk turnover of NTA substrates. Using protein steady-state  
51 and cycloheximide-chase degradation assays in yeast and Arabidopsis, we showed that  
52 turnover of ER-localised SQUALENE EPOXIDASE 1 (*AtSQE1*), a critical sterol biosynthesis  
53 enzyme, is mediated by *AtDOA10s*. Degradation of *AtSQE1* *in planta* did not depend on  
54 NTA, but Nt-acetyltransferases indirectly impacted its turnover in yeast, indicating kingdom-  
55 specific differences in NTA and cellular proteostasis. Our work suggests that, in contrast to  
56 yeast and mammals, targeting of Nt-acetylated proteins is not a major function of DOA10-  
57 like E3 ligases in Arabidopsis and provides further insight into plant ERAD and the  
58 conservation of regulatory mechanisms controlling sterol biosynthesis in eukaryotes.

59

60

61

62

63

64

65

66

67

68

69

70

71

72

73

74

## 75 Introduction

76

77 N-terminal (Nt) acetylation (NTA) is a highly prevalent chemical modification that is  
78 applied to around 60 % of cytosolic proteins in yeast and more than 80% in humans and  
79 plants (Arnesen et al. 2009; Bienvenut et al. 2012; Aksnes et al. 2015). NTA is performed by  
80 N-acetyltransferase (NAT) enzymes, which catalyse the transfer of an acetyl moiety from  
81 acetyl-CoA to the  $\alpha$ -amino group of specific Nt-residues in substrate proteins (Starheim et al.  
82 2012). In eukaryotes, most NTA is carried out co-translationally by five ribosome-anchored  
83 NATs (NATA-NATE), with experimentally determined substrate specificities in yeast,  
84 animals, and plants (Linster *et al.*, 2015, Aksnes *et al.*, 2019, Huber *et al.*, 2020).  
85 Furthermore, post-translational NTA also occurs in plants and animals via monomeric NATs  
86 that function away from the ribosome exit tunnel (Aksnes et al. 2019; Giglione and Meinel  
87 2021). These include membrane-bound NATF (Aksnes et al. 2015; Aksnes et al. 2017;  
88 Linster et al. 2020), a family of at least 6 plant-specific plastidic GNATs, that also catalyse  
89 lysine-acetylation (Dinh et al. 2015; Koskela et al. 2018; Bienvenut et al. 2020), and cytosolic  
90 NATH, which specifically Nt-acetylates actin in animals (Drazic et al. 2018; Wiame et al.  
91 2018).

92

93 The addition of an acetyl group has the effect of neutralising N-terminal charge and  
94 increasing hydrophobicity, which can influence protein fate in several ways, for example by  
95 promoting protein-protein interactions and directing protein localisation by increasing  
96 membrane affinity (Linster and Wirtz 2018; Ree et al. 2018). NTA also impacts protein  
97 folding, with deletions of NATA and particularly NATB causing the accumulation of misfolded  
98 protein aggregates in yeast (Friedrich et al. 2021). Furthermore, NTA has been shown to  
99 promote or prevent protein degradation depending on the protein target and cellular context.

100

101 In yeast and humans, acetylation of N-termini can destabilise certain proteins  
102 through the creation of Ac/N-degrons that target them for proteolysis via the acetylation-  
103 dependent (Ac/N)-degron pathway (Hwang et al. 2010; Park et al. 2015; Shemorry et al.  
104 2013). This degradation pathway was identified in yeast (*Saccharomyces cerevisiae*), where  
105 DEGRADATION OF ALPHA2 10 (DOA10) and NEGATIVE ON TATA-LESS 4 (NOT4) E3  
106 ligases were shown to function as Ac/N-recognins that target substrates via recognition of  
107 their Nt-acetylated N-termini (Hwang et al. 2010; Shemorry et al. 2013). Ac/N-degron  
108 pathway substrates have also been identified in humans (*Homo sapiens*), and are  
109 recognised by the human ScDOA10 homolog, MEMBRANE-ASSOCIATED RING-CH-TYPE  
110 FINGER 6 (MARCH6)/TEB4 (Nguyen et al. 2019; Park et al. 2015). In Arabidopsis  
111 (*Arabidopsis thaliana*), NTA of an MMD-initiating isoform of SUPPRESSOR OF NPR1,

112 CONSTITUTIVE 1 (SNC1) by NATA was shown to induce degradation, suggesting the  
113 Ac/N-degron pathway may also function in plants, though to date no plant Ac/N-recognins  
114 have been identified (Xu et al. 2015). Interestingly however, NTA of an alternative MD-  
115 initiating isoform of SNC1 by NATB was shown to have a stabilising effect, indicating that Nt-  
116 variants of the same protein can be differentially targeted for degradation (Xu et al. 2015;  
117 Gibbs 2015). Recently, the NATA-interacting HUNTINGTIN INTERACTING PROTEIN K  
118 (HYPK) protein in rice (*Oryza sativa*) was also shown to be degraded following N-terminal  
119 acetylation (Gong et al. 2022). Since most cellular proteins are Nt-acetylated, degradation  
120 via the Ac/N-degron pathway is proposed to be conditional, with substrates only degraded  
121 when their acetylated N-termini are not internalised within a protein's structure or shielded by  
122 a binding partner (Shemorry et al. 2013).

123

124 The discovery of the Ac/N-degron pathway partially conflicted with the historical view  
125 that NTA increases protein half-life by blocking ubiquitination of the N-terminus (Hershko et  
126 al. 1984). Recent studies have also suggested that NTA does not act as a broad or universal  
127 degradation signal. High throughput screening studies have independently shown that  
128 unstructured NTA reporter substrates of NATA and NATB were generally stable, and that  
129 mutations of NATA or NATB did not increase the abundance of their endogenous targets  
130 (Kats et al. 2018; Friedrich et al. 2021). Indeed, NTA has also been reported to block other  
131 Nt-processing events such as Met-excision, arginylation and the binding of N-recognins,  
132 thereby potentially protecting proteins from other degradative mechanisms such as the  
133 Arg/N-degron pathway (Kats et al. 2018; Park et al. 2015; Kim et al. 2014). One such protein  
134 is Arabidopsis SIGMA FACTOR-BINDING PROTEIN1 (SIB1), which is stabilised following  
135 NTA by NATB (Li et al. 2020). Kats *et al.* (2018) also observed that whilst mutation of  
136 ScDOA10 did stabilise many normally unstable reporter proteins, turnover of these peptides  
137 was largely defined by Nt-hydrophobicity rather than NTA itself. Additionally, in human cells,  
138 NTA by NATA was shown to protect nascent proteins from degradation by preventing their  
139 unwanted interaction with IAP E3 ligases that might otherwise trigger ectopic apoptosis  
140 (Mueller et al. 2021). Moreover, an analogous proteome-wide role for NTA in protein  
141 stabilisation was also recently uncovered in Arabidopsis, where stress-responsive NATA  
142 activity (Linster et al. 2015) was shown to mask non-Ac/N-degrons that would otherwise  
143 target NATA substrates for proteasomal degradation by as-yet-unknown E3 ligases (Linster  
144 et al. 2022; Gibbs et al. 2022).

145

146 The best characterised Ac/N-recognin, ScDOA10, is a RING-type E3 ligase that  
147 localises to the endoplasmic reticulum (ER) and nuclear envelope, and which was identified  
148 as a major component of the endoplasmic-reticulum-associated protein degradation (ERAD)

149 system that degrades misfolded ER proteins (Swanson et al. 2001). ScDOA10 is one of two  
150 ERAD E3 ligases and is primarily responsible for the ubiquitination of proteins with cytosolic  
151 degrons (ERAD-C) (Hirsch et al. 2009; Strasser 2018) although targeting of degrons within  
152 the ER membrane and retrotranslocase activity have also been reported for ScDOA10  
153 (Habeck et al. 2015; Schmidt et al. 2020). Two putative homologs of ScDOA10 have been  
154 identified in Arabidopsis: *AtDOA10A*, also known as ECERIFERUM9 (CER9)/  
155 SUPPRESSOR OF DRY2 DEFECTS1 (SUD1), and *AtDOA10B* (Liu et al. 2011). *Atdoa10a*  
156 mutants display a range of phenotypes, including altered cuticular wax composition,  
157 improved drought tolerance and ABA hypersensitivity during germination (Lu et al. 2012;  
158 Zhao et al. 2014). Mutations in *AtDOA10A* were also shown to repress the pleiotropic  
159 phenotypes caused by a point mutation in the sterol biosynthesis gene *SQUALENE*  
160 *EPOXIDASE 1 (SQE1)/ DROUGHT HYPERSENSITIVE2 (DRY2)* by downregulating 3-  
161 HYDROXY-3-METHYLGLUTARYL-COA REDUCTASE (HMGR), an upstream enzyme of the  
162 pathway (Doblas et al. 2013). It is still unclear if either *AtDOA10* homolog plays a major role  
163 in the plant ERAD system (Li et al. 2017; Huber et al. 2021). Furthermore, potential Ac/N-  
164 recognin functions for *AtDOA10s* have not yet been investigated and no physiological  
165 substrates of *AtDOA10s* have been identified.

166

167 Here, we sought to functionally characterise both putative *AtDOA10* orthologs with a  
168 view to establishing whether they function as Ac/N-recognin E3 ligases of the as-yet-  
169 uncharacterised Ac/N-degron pathway in plants. Our global and protein-specific results  
170 uncover a previously unknown function for *AtDOA10s* in the homeostatic regulation of sterol  
171 biosynthesis through controlling *AtSQE1* turnover, and suggests that their primary function in  
172 Arabidopsis is unrelated to the Ac/N-degron pathway and the bulk degradation of Nt-  
173 acetylated proteins.

174

175

176

## 177 **Results**

178

### 179 **Structure, functional conservation, and phylogeny of Arabidopsis DOA10-like** 180 **proteins**

181

182 To identify putative DOA10 homologs in Arabidopsis, we searched for protein  
183 sequences with homology to full-length ScDOA10 from *Saccharomyces cerevisiae*, which, in  
184 accordance with previous studies, identified two DOA10-like proteins encoded by the genes  
185 *At4g34100 (AtDOA10A/CER9/SUD1)* and *At4g32670 (AtDOA10B)* (Doblas et al. 2013; Lu et

186 al. 2012; Liu et al. 2011). These share 22.87% and 19.23% amino acid identity with  
187 ScDOA10, respectively, and 35.66% with each other (Fig.1a-b and Fig. S1). Identity is  
188 particularly high in the N-terminal RING-CH domain, an atypical variant of the classic RING  
189 domain that provides ubiquitin-ligase activity, and the TEB4/DOA10 (TD) domain, which  
190 influences interactions with the cognate ubiquitin conjugase 6 (UBC6) E2 enzyme in yeast  
191 (Fig.1b) (Doblas et al. 2013; Kreft and Hochstrasser 2011). Both AtDOA10s also have an  
192 extended C-terminal region containing 13-16 predicted transmembrane (TM) domains (Fig.  
193 S2a,b), similar to the experimentally confirmed 14 TM domains in ScDOA10 (Fig. 1a) (Kreft  
194 et al. 2006).

195 To determine whether AtDOA10A and AtDOA10B represent functional homologs of  
196 ScDOA10, we assessed their capacity to complement the yeast *Scdoa10Δ* mutant. We  
197 cloned both proteins as C-terminal GFP fusions driven by the *GPD* promoter, transformed  
198 them into *Scdoa10Δ*, and confirmed expression using RT-PCR (Fig. 1c). In growth assays,  
199 *Scdoa10Δ* displayed relative insensitivity to hygromycin, which was reverted in mutants  
200 expressing AtDOA10A-GFP (to a greater extent than WT yeast, possibly due to over  
201 expression of the transgene), but unaffected in lines expressing AtDOA10B-GFP (Fig. 1d).  
202 Thus, AtDOA10A, but not the C-terminally truncated AtDOA10B (Fig. 1a), is able to  
203 compensate for the loss of endogenous ScDOA10 activity in yeast, indicating at least partial  
204 conservation of function for this putative ortholog.

205 To understand the nature of the Arabidopsis DOA10 gene duplication, we  
206 constructed a phylogenetic tree of DOA10-like protein sequences identified via BLASTP  
207 from a range of diploid flowering plant genomes, including diverse monocots, dicots and  
208 several members of the *Brassicaceae* family (Fig. 1e). We found that many, though not all,  
209 plant species had two DOA10-like proteins. Whilst most DOA10-like sequences clustered  
210 into defined branches that split the monocots and dicots, AtDOA10B was part of a separate  
211 *Brassicaceae*-specific clade, grouping with similar DOA10B-like sequences from lyre-leaved  
212 rock cress (*Arabidopsis lyrata*), field mustard (*Brassica rapa*) and pink shepherd's-purse  
213 (*Capsella rubella*). In contrast, where two putative orthologs were identified in other species,  
214 both sequences occurred together in species-specific pairs within the main AtDOA10A-like  
215 clade - e.g., pineapple (*Ananas comosus*), poplar (*Populus trichocarpa*), and soybean  
216 (*Glycine max*). This suggests that the truncated DOA10B-like variant emerged in the  
217 *Brassicaceae* lineage.

218

219 **AtDOA10A and AtDOA10B are broadly expressed and localise to the endoplasmic**  
220 **reticulum**

221

222 We developed transgenic lines expressing C-terminal GUS fusions of *AtDOA10s*  
 223 driven by 2kb of the endogenous promoter (*pAtDOA10A/B::AtDOA10A/B-GUS*).  
 224 Histochemical staining revealed that both proteins are broadly detectable in 7-day and 14-  
 225 day old seedlings, particularly in roots, which showed enrichment in the primary root  
 226 meristem, lateral root primordia and vasculature (Fig. 2a). A complementary RT-qPCR  
 227 analysis of relative *AtDOA10A/B* mRNA abundance also identified transcripts for both  
 228 proteins across a range of seedling and adult tissues, suggesting broad roles for *AtDOA10s*  
 229 in diverse cell types (Fig. 2b). Corroborating the reduced levels of *AtDOA10B-GUS* staining  
 230 relative to *AtDOA10A-GUS*, *AtDOA10B* mRNA abundance was much lower than *AtDOA10A*  
 231 (approx. 20-fold) across all tissue types.

232 To determine *AtDOA10* subcellular localisation, we isolated total protein from the  
 233 *pAtDOA10A/B::AtDOA10A/B-GUS* transgenics and prepared soluble and microsomal  
 234 fractions. Anti-GUS immunoblotting revealed exclusive enrichment of *AtDOA10A/B-GUS* in  
 235 the microsomal fractions, alongside the known ER marker Calnexin (CNX) 1/2 (Fig. 2c). We  
 236 also examined the subcellular localisation of an eYFP-*AtDOA10A* transgene in transiently  
 237 transformed *Nicotiana benthamiana* leaf epidermal cells. Here, eYFP-*AtDOA10A* co-  
 238 localised with the ER marker *AtVMA12-RFP* (Fig. 2d). Thus, *AtDOA10s* are ER-localised,  
 239 like yeast *ScDOA10* and human MARCH6/TEB4.

240

## 241 **Generation and phenotypic assessment of *AtDOA10A* and *B* mutants**

242

243 We obtained homozygous *Atdoa10a* and *Atdoa10b* T-DNA insertional mutants and  
 244 confirmed the knockouts by RT-PCR (Fig. 3a and Fig. S3a). Although only *AtDOA10A* was  
 245 able to complement *Scdoa10Δ*, we postulated that both *AtDOA10s* could have overlapping  
 246 or redundant functions in Arabidopsis. As such, we attempted to make a double mutant, but  
 247 the proximity of the two genes (separated by 0.57 Mb) meant that a crossover event was  
 248 likely to be very rare; in accordance with this, we were unable to identify any double mutants  
 249 and instead took an RNAi approach. We designed two different RNAi constructs that  
 250 targeted the first and second exons of *AtDOA10B* (Fig. 3a) and transformed these into  
 251 *Atdoa10a*. RT-qPCR analysis of the derived progeny led to the identification of two  
 252 independent lines with reduced *AtDOA10B* mRNA (~50% Col-0 levels): *Atdoa10a/b RNAi 3-*  
 253 *7* and *RNAi 4-2* (Fig. 3b). Despite screening several lines, we did not identify any with  
 254 stronger depletion.

255 No major phenotypic differences between lines were observed when grown under  
 256 standard conditions, though mutant rosettes were slightly smaller than WT rosettes, in  
 257 accordance with previous observations for *Atdoa10a* (Fig. 3c) (Huber et al. 2021).  
 258 *AtDOA10A* was previously linked to ABA signalling and the control of cuticle development,



259 with *Atdoa10a* mutants displaying seed ABA hypersensitivity and drought tolerance  
260 phenotypes (Zhao et al. 2014; Lu et al. 2012). We also observed ABA hypersensitivity of  
261 *Atdoa10a* seeds (Fig. 3d), and showed that WT sensitivity was restored in *Atdoa10a* lines  
262 complemented with *pDOA10A::AtDOA10A-YFP* (Fig. S3b). In contrast, the *Atdoa10b* single  
263 mutant had no obvious phenotype, and ABA sensitivity of *Atdoa10a/b RNAi 4-2* resembled  
264 that of the *Atdoa10a* single mutant, suggesting that *AtDOA10A* and *AtDOA10B* do not have  
265 additive or redundant roles in ABA-related responses.

266

### 267 **RNA-seq and Nt-acetylome profiling indicate that *AtDOA10s* do not regulate global** 268 **turnover of Nt-acetylated proteins**

269

270 We carried out an RNA-seq analysis of 10-day old *Atdoa10a/b RNAi 4-2* seedlings  
271 grown under long day conditions, which identified 447 differentially expressed genes (DEGs;  
272 217 up, 230 down) relative to Col-0 (False Discovery Rate (FDR) adjusted p-value ( $q$ ) $<0.05$ )  
273 (Fig. 4a and Supplemental dataset 1). Amongst these, 89 had a fold-change of two or more.  
274 This modest number of DEGs likely reflects the fact that plants were grown under ambient,  
275 non-stressed conditions. Nonetheless, Gene Ontology (GO) analysis uncovered several  
276 enriched GO-terms that are consistent with potential roles for *AtDOA10s* in protein quality  
277 control or ERAD, including: cellular component term *perinuclear region of the cytoplasm*  
278 (18.1 fold enrichment,  $2.05E-07$  FDR); biological process terms *protein folding* (4.63  
279 enrichment,  $6.31E-03$  FDR) and *protein refolding* (fold enrichment 10.18,  $1.50E-02$  FDR),  
280 and; molecular function term *unfolded protein binding* (5.14 fold enrichment,  $1.61E-02$  FDR).  
281 We also carried out RNA-seq analysis on 10-day old NAT-depleted plants: *amiNAA10* (i.e.,  
282 *NATA*) knockdown and *Atnaa20* (i.e., *NATB*) mutant seedlings. We hypothesised that there  
283 might be some overlap in the transcriptome of *Atdoa10a/b* and *nat* mutants, due to shared  
284 ectopic stabilisation of Ac/N-degron protein targets. As expected, given *NATA*'s role in  
285 acetylating 40% of cytosolic proteins, *amiNAA10* seedlings had the greatest number of  
286 DEGs (7,139), with *Atnaa20* having fewer (2,486). Interestingly, nearly 70% of the  
287 *Atdoa10a/b RNAi* annotated DEGs (307/444) were also differentially expressed in either  
288 NAT-mutant transcriptome (Fig. 4b), with 75% of *Atdoa10a/b-amiNAA10* and 78% of  
289 *Atdoa10a/b-naa20* shared DEGs occurring in the same direction (i.e., up in both or down in  
290 both; supplementary dataset S1).

291

292 If *AtDOA10s* function as general Ac/N-recognins of the Ac/N-degron pathway, an  
293 accumulation of Nt-acetylated proteins would be expected in plants lacking *AtDOA10*  
294 function compared to Col-0. This could manifest as either an increase in the total levels of  
295 Nt-acetylated proteins, or increased ratio of acetylated to non-acetylated variants of a

296 particular protein(s). We performed quantitative Nt-acetylome profiling on total protein  
297 extracts from both Col-0 and *doa10a/b RNAi 4-2* seedlings using the “stable isotope labelling  
298 protein N-terminal acetylation quantification (SILProNAQ)” method (Bienvenut et al. 2017a),  
299 with data processed using the EnCOUNTER tool (Bienvenut *et al.*, 2017b) (Supplemental  
300 dataset 2). A total of 651 and 594 N-termini were identified in Col-0 and *Atdoa10a/b RNAi 4-*  
301 *2*, respectively, with 426 common to both lines (Fig. 4c and d). In both genotypes,  
302 approximately half of these N-termini were Nt-acetylated (48% in Col-0 and 49% in  
303 *Atdoa10a/b*). We were able to quantify a total of 342 unique N-termini (277 in Col-0 and 256  
304 in *Atdoa10a/b RNAi 4-2*). In Col-0 58% (161/277) were either fully or partially acetylated,  
305 which was similar to 59% observed for *Atdoa10a/b RNAi 4-2* (151/256). Global NTA  
306 variation comparisons based on either N-terminal position (Fig. 4e) or cellular sub-  
307 compartment (Fig. S4) showed no differences in overall NTA level in *Atdoa10a/b RNAi 4-2*  
308 vs Col-0, and a similar distribution in NTA-frequency was observed for all natural amino  
309 acids at the N-terminal position (Fig. 4f). Moreover, relative quantification of Nt-acetylated  
310 peptides shared between *Atdoa10a/b RNAi 4-2* and WT identified no proteins with  
311 significantly (i.e., FDR<5%) increased or decreased NTA (Fig. 4g). Collectively, these Nt-  
312 profiling findings suggest that strong depletion of AtDOA10 levels does not affect the overall  
313 turnover of Nt-acetylated proteins.

314

315

### 316 **Proteolytic turnover of AtSQE1 requires AtDOA10A and AtNAA20 in heterologous** 317 **yeast degradation assays**

318

319 Whilst the *Atdoa10a/b RNAi 4-2* double mutant had no clear differences in global  
320 NTA, AtDOA10s could still play a role in targeting specific Nt-acetylated protein substrates  
321 for degradation. We took a targeted approach to identify a potential physiological substrate  
322 to use for investigating protein turnover in finer molecular detail. Mutations in AtDOA10A  
323 were previously shown to suppress phenotypic defects in the *dry2* mutant, which lacks  
324 SQE1 activity. Here, defects arise due to a build-up of toxic intermediates, and a secondary  
325 mutation in AtDOA10A alleviates this by downregulating HMGR enzyme activity, which  
326 functions several steps ahead of squalene synthesis (Doblas et al. 2013). Moreover, in  
327 yeast and mammals, SQE homologs (Ergosterol Biosynthesis 1 (ERG1) in yeast and  
328 squalene monooxygenase (SM) in mammals) localise to the ER membrane and are direct  
329 proteolytic targets of ScDOA10 and HsMARCH6/TEB4, respectively (Foresti et al. 2013;  
330 Sharpe et al. 2020; Zelcer et al. 2014). Similarly, Arabidopsis SQE1 is predicted to have  
331 transmembrane regions and localise to the ER, although it does not contain a predicted N-

332 terminal secretory signal peptide (Fig. S2 c,d). Given the evolutionary conservation of  
333 DOA10-like E3 ligases and their roles in modulating sterol biosynthetic pathways, we  
334 postulated that Arabidopsis SQE1 turnover might also be regulated by AtDOA10s.

335 We used WT and mutant yeast strains as a heterologous system for expressing  
336 AtSQE1 and monitoring its stability by immunoblotting. Steady-state levels of AtSQE1-HA  
337 were higher in *Scdoa10Δ* than WT yeast, and this could be reverted when AtSQE1-HA was  
338 co-expressed with AtDOA10A-YFP, but not AtDOA10B-YFP (Figs. 5a and b). Next, we  
339 monitored AtSQE1-HA turnover rates using cycloheximide (CHX) chase assays, which  
340 revealed rapid degradation of AtSQE1-HA in WT yeast cells, but relative stabilisation in  
341 *Scdoa10Δ* (Fig. 5c). Moreover, the enhanced stability was partially reverted when  
342 AtDOA10A-YFP was co-transformed into *Scdoa10Δ* (Fig. 5d).

343 AtSQE1 initiates with the residues Met-Glu- (ME-) and should retain its initiator Met  
344 during translation and be targeted by ribosome-associated NATB (comprising NAA20  
345 catalytic and NAA25 auxiliary subunits) (Aksnes et al. 2019). It was previously shown that  
346 99% of ME-initiating proteins undergo NTA in humans (Aksnes et al. 2016), with similarly  
347 high numbers in yeast and Arabidopsis (Fig. S5 and Supplemental Dataset 3). It was also  
348 shown that human *HsNAA20* can complement Arabidopsis *Atnaa20* mutants, but that yeast  
349 *ScNAA20* cannot (Huber et al. 2020). Whether AtNAA20 can compensate for loss of  
350 ScNAA20 function is unknown. To investigate whether AtSQE1-HA turnover is mediated by  
351 Nt-acetylation and the Ac/N-degron pathway, we also monitored AtSQE1-HA stability in the  
352 yeast *Scnaa20Δ* mutant (Fig. 5c and e). Similar to *Scdoa10Δ*, and potentially consistent  
353 with the Ac/N-degron pathway, we saw strong enhancement of AtSQE1-HA stability relative  
354 to WT, which was almost completely reverted when AtNAA20 was co-expressed. This  
355 indicates that NATB activity is required for AtSQE1 turnover and reveals that Arabidopsis  
356 AtNAA20 can functionally replace ScNAA20.

357

### 358 **Impact of N-terminal mutagenesis on AtSQE1 stability suggests indirect effects of Nt-** 359 **acetyltransferases on protein turnover in yeast**

360

361 To further investigate the connection between NTA and AtSQE1 degradation, we  
362 developed a series of Nt-mutagenized variants of AtSQE1 that are predicted to be blocked  
363 for NTA, or which are targeted by different cognate NATs (Fig. 6a, Fig. S5 and Supplemental  
364 dataset 3): (1) MP-SQE1, which should undergo Met-excision by methionine  
365 aminopeptidases (MetAPs) but no further Nt-acetylation, as Nt-Proline residues are not  
366 acetylated (Goetze et al. 2009); (2) MK-SQE1, which should be rarely acetylated (Arnesen  
367 et al. 2009), and (3) MA-SQE1, which would instead be Nt-acetylated by NATA/NAA10  
368 following initiator Met removal by MetAP. We hypothesised that MP- and MK-SQE1-HA

369 would be stable in WT yeast if turnover is dependent on NTA, but instead found that their  
370 steady-state levels were in fact reduced relative to WT ME-AtSQE1-HA (Fig. 6b), perhaps  
371 due to codon differences impacting translation (Kozak 1997). Moreover, when expressed in  
372 *Scdoa10Δ*, relative abundance increased for all proteins, but the ratios between them were  
373 maintained, suggesting that ScDOA10 targets all three Nt-variants and that their direct NTA  
374 is not critical for degradation.

375 In accordance with these steady-state analyses (Fig. 6b), we found that mutant MP-  
376 AtSQE1-HA rapidly degraded following CHX treatment, similarly to WT ME-AtSQE1-HA (Fig.  
377 6c). We also observed stabilisation of WT ME-AtSQE1-HA in *Scnaa10Δ* mutant cells (Fig.  
378 6d), which lack a functional NATA enzymatic complex; this was unexpected, since ME- is  
379 not a target sequence for NATA activity. Finally, we examined the stability of mutant MA-  
380 AtSQE1-HA, where the N-terminus is remodelled from a NATB to a NATA target. Like all  
381 other variants, MA-AtSQE1-HA was unstable in WT yeast, but was surprisingly still stable in  
382 the non-cognate *Scnaa20Δ* mutant in addition to *Scdoa10Δ* (Fig. 6e,f). Collectively, these  
383 assays indicate that degradation of AtSQE1 via DOA10 in yeast is indirectly influenced by  
384 NATA and NATB activity.

385

### 386 **Nt-acetylation-independent turnover of AtSQE1 by AtDOA10 in Arabidopsis**

387

388 To test AtSQE1 stability *in planta*, we generated a range of stable transgenic  
389 Arabidopsis lines expressing Nt-variants of AtSQE1-Myc driven by the constitutive 35S  
390 CaMV promoter. WT ME-AtSQE1-Myc was expressed in Col-0, *Atdoa10a*, *Atdoa10b*,  
391 *Atdoa10a/b RNAi 4-2* and *Atnaa20*, whilst mutant non-acetylatable MP-AtSQE1-Myc was  
392 expressed in Col-0 only. For each construct we identified two independent transgenics and  
393 confirmed their expression by RT-qPCR (Fig. S6a). Both the ME- and MP- Nt-variants of  
394 AtSQE1-Myc localised to the ER in Col-0 (Fig. 7a). Thus, AtSQE1 resides in the same  
395 cellular compartment as AtDOA10s (like in yeast and mammals), and the introduced E2P N-  
396 terminal mutation does not disrupt this subcellular targeting. CHX chase assays revealed  
397 that WT ME-AtSQE1-Myc was unstable after 24 h of translational shutdown with CHX in all  
398 genetic backgrounds tested, except for the *Atdoa10a/b RNAi 4-2* double mutant (Fig 7b).  
399 This was consistent across two independent transgenic lines (Fig. 7b and Fig. S6b). A  
400 shorter CHX experiment corroborated this finding, showing that WT ME-AtSQE1-Myc is  
401 turned over in WT within 6 h, but remains stable in the *Atdoa10a/b RNAi 4-2*, or if co-  
402 incubated with proteasome inhibitor bortezomib (Fig 7c and Fig. S6c). Mutant MP-AtSQE1-  
403 Myc was also unstable in Col-0 (Fig 7b). These data reveal that proteasomal degradation of  
404 AtSQE1 requires both AtDOA10 proteins *in planta* and that this turnover is neither

405 dependent on indirect NAT activity (in contrast to yeast; Figs 5 and 6) nor direct NTA of  
406 AtSQE1 by NATB.

407 Potentially consistent with the fact that AtSQE1 accumulates in *Atdoa10a/b RNAi 4-*  
408 *2*, we observed extreme epinasty in seedlings of this mutant relative to Col-0, a phenotype  
409 that has previously been shown to coincide with altered sterol biosynthesis (Fig. 7d)  
410 (Carland et al. 2010). Precise control of sterol synthesis pathway enzymes is required to  
411 regulate and maintain appropriate levels of phytosterols and their intermediates in  
412 Arabidopsis (De Vriese et al. 2021). In human and yeast systems, SQE expression and  
413 stability are influenced by the accumulation or consumption of different sterols and pathway  
414 intermediates, but how such feedback works in Arabidopsis is currently unknown (Foresti et  
415 al. 2013; Gill et al. 2011; Scott et al. 2020; Leber et al. 2001). We investigated whether  
416 chemical inhibition of Arabidopsis sterol synthesis impacts AtSQE1 stability via AtDOA10s  
417 through treating seedlings with the chemical lauryldimethylamine oxide (LDAO), a dual  
418 inhibitor of both the cycloartenol synthase (CAS) enzymes, which cyclise 2,3-oxidosqualene  
419 (the direct product of AtSQE1) to produce cycloartenol, and cycloeucaenol cycloisomerase  
420 (CPI) enzymes, which act further downstream (Darnet et al. 2020). We observed extremely  
421 rapid turnover of ME-AtSQE1-Myc protein in response to LDAO treatment, occurring within  
422 just 30 minutes (Fig. 7e). This was specific to ME-AtSQE1-Myc and not a consequence of  
423 general protein turnover nor ER disruption due to LDAO's detergent properties, since ER-  
424 localised CNX1/2 proteins were unaffected. Interestingly however, LDAO was still able to  
425 induce rapid turnover of ME-AtSQE1-Myc in *Atdoa10a/b RNAi 4-2* (Fig. 7e). We also directly  
426 inhibited AtSQE1 using terbinafine, a non-competitive inhibitor of squalene epoxidase  
427 enzymes (Nowosielski et al. 2011); this led to strong accumulation of AtSQE1-Myc (Fig. 7f),  
428 likely caused by positive feedback through reduced degradation given that expression was  
429 driven by the constitutive 35S CaMV promoter.

430

## 431 Discussion

432

433 In yeast and humans, DOA10 E3 ligases function as Ac/N-recognins that target  
434 functionally diverse proteins for degradation via recognition of their acetylated N-termini  
435 (Park et al. 2015; Hwang et al. 2010; Shemorry et al. 2013). In plants, the Ac/N-degron  
436 pathway and its associated Ac/N-recognins are yet to be characterised, although it was  
437 previously shown that NTA of rice HYPK and a specific Nt-isoform of Arabidopsis SNC1  
438 triggers their degradation (Xu et al. 2015; Gong et al. 2022). Whilst HYPK and SNC1 are  
439 potential plant Ac/N-degron pathway targets, the Arabidopsis SIB1 protein was recently

440 shown to be stabilised by NATB-mediated NTA (Li et al. 2020). Moreover, large-scale  
441 studies in yeast, humans and plants have established broader roles for NTA in proteome  
442 stabilisation (Kats et al. 2018; Friedrich et al. 2021; Mueller et al. 2021; Linster et al. 2022;  
443 Gibbs et al. 2022). Therefore, the relationship between protein NTA and degradation is  
444 complex, and is likely to vary depending on protein identity and cellular context. Here, we  
445 investigated Arabidopsis *AtDOA10*-like E3 ligases, focussing specifically on their potential  
446 function as Ac/N-recognins. Nt-acetylome profiling revealed no apparent differences in the  
447 accumulation of Nt-acetylated proteins in *Atdoa10a/b RNAi* vs Col-0, suggesting that  
448 depletion of *AtDOA10* proteins does not influence the bulk turnover of Nt-acetylated  
449 proteins. However, the proteins identified and quantified in our comparative Nt-acetylome  
450 analysis represent only a small proportion of total potential Ac/N-degron substrates, which  
451 means we cannot rule out that *AtDOA10*s may have specific roles in targeting a more  
452 constrained set of Nt-acetylated proteins. Alternatively, other E3 ligases, for example,  
453 putative orthologs of the NOT4 Ac/N-recognins (Shemorry et al. 2013; Gibbs et al. 2016),  
454 may function as primary Ac/N-recognins in plants.

455 We identified the ER-resident *AtSQE1* protein, a rate-limiting enzyme in the sterol  
456 biosynthesis pathway (Rasbery et al. 2007), as a target of *AtDOA10*s. Turnover of *AtSQE1*  
457 requires functional *AtDOA10*s and was not linked to acetylation of its N-terminus *in planta*,  
458 since its stability was unaltered when its putative cognate NAT, NATB, was deleted (Fig. 7b).  
459 Surprisingly however, we found that *AtSQE1* stability was indirectly influenced by NAT  
460 activity when heterologously expressed in yeast. Partial or complete NATA or NATB  
461 inactivation led to enhanced stabilisation regardless of the Nt-variant being assayed (Figs 5  
462 and 6), which may be due to indirect effects on other proteins linked to translational or  
463 proteolytic machineries; the ERAD protein *ScDer1*, for example, requires NTA by NATB for  
464 stability (Zattas et al. 2013). Our cross-kingdom analysis of *AtSQE1* stability has therefore  
465 uncovered differences in the ways in which NTA can influence proteostasis in yeast and  
466 plants, suggesting that caution should be applied when investigating the connection between  
467 NTA and protein turnover, and particularly when extrapolating between organisms.

468 In contrast to yeast and humans, the Arabidopsis genome encodes for two *DOA10*-  
469 like E3 ligases. *AtDOA10A*, but not *AtDOA10B*, was able to complement *Scdoa10Δ* yeast,  
470 with respect to both hygromycin sensitivity and turnover of heterologously expressed  
471 *AtSQE1* (Figs. 1 and 5). Whilst both *AtDOA10*s are smaller than *ScDOA10*, *AtDOA10B* is  
472 particularly truncated (Fig. 1a), and appears to be restricted to the Brassicaceae clade (Fig.  
473 1e), which could explain its inability to complement *Scdoa10Δ*. This may be the result of  
474 incompatibility between *AtDOA10B* and components of the endogenous yeast ubiquitination  
475 machinery, since in Arabidopsis *AtSQE1* degradation was only inhibited in the *Atdoa10a/b*

476 *RNAi* double mutant. Despite this example of functional redundancy, other evidence points  
477 to additional paralog-specific activities. For instance, *Atdoa10a* single mutants display a  
478 range of phenotypes that do not manifest in *Atdoa10b*, and which are not amplified in  
479 *Atdoa10a/b RNAi* lines, including altered cuticular wax composition and strong ABA  
480 hypersensitivity (Fig. 3d) (Lu et al. 2012; Zhao et al. 2014).

481 DOA10s in yeast and humans are major E3 ligases of the ERAD system (Ravid et al.  
482 2006), whilst roles for AtDOA10s in the Arabidopsis ERAD system are still unclear (Liu et al.  
483 2011; Huber et al. 2021; Li et al. 2017). This may be due to functional redundancy, a  
484 concept supported by our observations that turnover of ER-resident AtSQE1 is dependent  
485 on both AtDOA10s. Interestingly though, AtDOA10B was shown to physically associate with  
486 the ERAD-associated ubiquitin-conjugase 32 (UBC32) (Cui et al. 2012), and be  
487 transcriptionally induced by L-azetidine-2-carboxylic acid (AZC), a proline analogue that  
488 causes protein misfolding (Kim et al. 2017). We also observed significant upregulation of  
489 AtDOA10B, but not AtDOA10A, in response to the ERAD elicitor tunicamycin (Fig. S7). This  
490 suggests that AtDOA10s have both redundant and distinct roles linked to different cellular  
491 processes, and that the AtDOA10B paralog may have evolved to take on a more prominent  
492 role in stress-associated, rather than constitutive, ERAD in Arabidopsis. Further analysis of  
493 the transcriptomic, proteomic, and physiological response of *Atdoa10a* and *b* mutants to ER-  
494 and protein misfolding stresses will shed further light on the roles these proteins play in  
495 ERAD and protein homeostasis.

496 Sterol biosynthesis is sensitive to fluctuations in enzyme activity and substrate  
497 availability at each stage. For example, a build-up of cholesterol in animals feeds back to  
498 downregulate the pathway and redirect precursor flux, whilst increases in lanosterol  
499 abundance has a similar effect in yeast (Gill et al. 2011; Scott et al. 2020; Foresti et al.  
500 2013). In plants, a build-up of squalene and/or its precursors is toxic but can be  
501 counteracted by a reduction of HMGR enzyme activity, which is enhanced when *AtDOA10A*  
502 is knocked out (Doblas et al. 2013). Our LDAO assays reveal that ectopic build-up of  
503 downstream sterol intermediates also triggers feedback mechanisms to downregulate sterol  
504 production in plants, in this case promoting *AtSQE1* destabilisation, possibly through an  
505 alternative E3 ligase or an autophagic mechanism (Fig. 7e). In contrast, direct inhibition of  
506 *AtSQE1* with terbinafine led to increased accumulation of *AtSQE1* (Fig. 7f). Interestingly,  
507 *ScDOA10* was previously shown to target multiple enzymes of the sterol biosynthesis  
508 pathway in yeast, indicating that it is a master regulator of this biochemical pathway (Scott et  
509 al. 2020). The fact that *AtDOA10s* influence both HMGR activity and *SQE1* stability also  
510 points to central functions for DOA10s in coordinating sterol production at several steps in  
511 plants (Fig. 8). Whether *AtDOA10s* control turnover of other Arabidopsis *SQEs* (Rasbery et  
512 al. 2007), remains to be determined, though the Brassicaceae-specific *AtSQE5* (Laranjeira

513 et al. 2015) was significantly downregulated in the *Atdoa10a/b RNAi 4-2* transcriptome,  
514 potentially suggesting negative feedback. Furthermore, direct interaction and ubiquitination  
515 of AtSQE1 by AtDOA10s needs to be confirmed biochemically. A more detailed analysis of  
516 the connection between AtDOA10s, AtSQEs and other components of the sterol synthesis  
517 pathway in Arabidopsis will provide further insight into the complexities of sterol homeostasis  
518 in plants.

519 To conclude, our work suggests that DOA10-like E3 ligases, in contrast to their  
520 putative yeast and mammalian homologs, do not play a major role in the degradation of Nt-  
521 acetylated proteins in Arabidopsis, suggesting that the plant Ac/N-degron pathway is less  
522 highly conserved across kingdoms than other N-degron pathways, and that its E3 ligase  
523 component(s) await discovery. Furthermore, we uncover conservation of a DOA10-SQE  
524 regulatory module across 1.5 billion years of evolution, which suggests that homeostatic  
525 mechanisms controlling sterol biosynthesis have ancient origins.

526

## 527 **Materials and Methods**

528

### 529 **Arabidopsis growth conditions and transgenic lines**

530 Arabidopsis (*Arabidopsis thaliana*) lines were obtained from the Nottingham  
531 Arabidopsis Stock Centre (NASC), apart from *amiNAA10* and *naa20* (Huber et al. 2020;  
532 Linster et al. 2015). *AtDOA10A/B-GUS/YFP* transgenics were produced by cloning the  
533 genomic sequences of *AtDOA10A/B* (At4g34100 and At4g32670), including ~2 kb of  
534 upstream sequence, into the Gateway® entry vectors pDONR™221/pENTR™/D-TOPO™  
535 (Invitrogen) before ligation into pGWB533/pGWB540 (Nakagawa et al. 2007). *AtDOA10B*  
536 RNAi target sequences were cloned into pK7GWIWG2(I) (Karimi et al. 2002). The *AtSQE1*  
537 (At1G58440) CDS was cloned into pENTR™/D-TOPO™ (Invitrogen) and subsequently  
538 pGWB17 (Nakagawa et al. 2007) to produce *35S::AtSQE1-Myc*; the E2P mutation was  
539 introduced via a mismatched forward primer. Expression clones were transformed into  
540 *Agrobacterium tumefaciens* (GV3101 pMP90) for Arabidopsis transformation via floral dip  
541 (Zhang et al. 2006). All cloning and genotyping primers are listed in Supplementary Table 1.

542

543 Arabidopsis plants were grown on soil (Levington M3 compost, vermiculite and  
544 perlite; 4:2:1 ratio), in long day (16 h light at 22°C) or short day (8 h light at 22°C) conditions.  
545 For sterile growth, seeds were surface sterilised (10% v/v bleach), plated onto half-strength  
546 Murashige & Skoog (½ MS) medium (1% w/v agar, pH 5.7), stratified at 4°C for 48 hours  
547 and grown in long days. ABA (Sigma Aldrich) was added directly into the ½ MS growth  
548 medium to the appropriate concentration. LDAO (Cayman Chemical Company) treatments  
549 were carried out on 7-day old seedlings in water supplemented with 100 µg ml<sup>-1</sup> LDAO.



550 Terbinafine hydrochloride (20 $\mu$ M) (Sigma-Aldrich) was applied to seedlings in the same  
551 manner as cycloheximide (see below). All experiments involving chemical treatment of  
552 *Arabidopsis* were conducted at least three times.

553

#### 554 **Yeast assays**

555 Yeast (*Saccharomyces cerevisiae*) cells used were homozygous diploid BY4743  
556 cells derived from the S288C strain (Dharmacon yeast KO collection, Horizon Discovery).  
557 Yeast were transformed with *AtDOA10A*, *AtDOA10B* and *AtNAA20* (At1g03150) in the  
558 pAG416GPD-ccdB-EGFP vector (Addgene plasmid #14196, Susan Lindquist) and *AtSQE1*  
559 in the pAG413GPD-ccdB-HA vector (Addgene plasmid #14238, Susan Lindquist), or the  
560 corresponding empty vectors. Transformation was performed by the lithium acetate method:  
561 A 1 $\mu$ l loop of cells was added to 2 $\mu$ g of expression clone and 100 $\mu$ l of transformation buffer  
562 (33% v/v polyethylene glycol 3350, 0.33M lithium acetate, 0.66% v/v  $\beta$ -mercaptoethanol).  
563 Cells were briefly vortexed, incubated at 37°C for 45 minutes (200rpm), then spread on  
564 synthetic drop-out (DO) media (Formedium) and incubated at 30°C. Non-transformed cells  
565 were grown on yeast-extract peptone dextrose (YPD). G418 (Sigma-Aldrich) was added to  
566 media used for the growth of mutant strains. For hygromycin treatments, cells were grown  
567 overnight in liquid DO media and diluted to an OD<sub>600</sub> of 1.0. A serial dilution of each culture  
568 was then spotted onto plates containing DO media with added hygromycin B (TOKU-E) (50-  
569 75 $\mu$ g ml<sup>-1</sup>).

570

#### 571 **Reverse transcription PCR (RT-PCR) and reverse transcription quantitative PCR (RT- 572 qPCR)**

573 RNA was extracted from snap-frozen samples using an RNeasy minikit (QIAGEN)  
574 and analysed by NanoDrop™ 1000 spectrophotometer (ThermoFisher Scientific). 1.5 $\mu$ g of  
575 RNA was treated with RQ1 DNase (Promega) and cDNA was synthesised using oligo(dT)  
576 primers and SuperScript™ II Reverse Transcriptase (ThermoFisher Scientific). For semi-  
577 quantitative RT-PCR, synthesised cDNA was used in PCR reactions specific to the gene of  
578 interest and *ACTIN7*. RT-qPCR was performed on 45ng template cDNA using Brilliant III  
579 Ultra-Fast SYBR® Green QPCR Master Mix with Low ROX (Agilent), using an AriaMx Real-  
580 time PCR System (Agilent). Relative expression was calculated using the 2<sup>- $\Delta$  $\Delta$ CT</sup> method  
581 (Livak and Schmittgen 2001) normalised to *ACTIN7*. All primers used are listed in  
582 Supplementary Table S1.

583

#### 584 **Phylogenetic tree construction**

585 Putative DOA10-like protein sequences were identified by BLASTP at NCBI using  
586 ScDOA10 as the template sequence. Sequences were aligned in SEAVIEW5 using the

587 Clustal O method and the phylogenetic tree was constructed using SEAVIEW5 and  
588 BIONJ (Bio Neighbour-Joining) method (Gouy et al. 2021), where Poisson Correction and  
589 bootstrap testing is performed with 1000 iterations.

590

### 591 **Histochemical staining**

592 Arabidopsis seedlings were incubated in GUS stain solution (100mM phosphate  
593 buffer (pH 7.0), 2mM X-gluc (X-GLUC Direct) 0.1% v/v Triton-X-100, 1mM potassium  
594 ferricyanide, 1 mM potassium ferrocyanide) at 37°C for 24 hours. Seedlings were cleared  
595 and fixed in 3:1 ethanol:acetic acid, mounted onto microscope slides in 50% v/v glycerol and  
596 imaged on a dissecting microscope. At least three biological repeats were conducted for  
597 each transgenic line.

598

### 599 **Cell Fractionation**

600 Cell fractionation was performed based on Abas & Luschnig (2010). Tissue was  
601 lysed by grinding in extraction buffer (100 mM Tris-HCl (pH 8.0), 5% v/v glycerol, 10 mM  
602 EDTA, 10mM EGTA, 5mM KCl, 1mM DTT) supplemented with cComplete™, Mini, EDTA-free  
603 Protease Inhibitor Cocktail (Roche), and precleared by centrifugation at 630xg (10 minutes).  
604 High-speed centrifugation (21000xg) was then carried out for 2 hours (4°C) to pellet the  
605 microsomal fraction. The supernatant (soluble fraction) was removed for analysis, the pellet  
606 washed with 150µl of wash buffer (100mM Tris-HCl (pH 8.0), 5mM EDTA, 150mM NaCl) and  
607 resuspended in buffer (10mM Tris-HCl (pH 8.0), 0.5mM EDTA, 150mM NaCl). A 1/5<sup>th</sup>  
608 volume of 5x sample buffer (300mM Tris-HCl (pH 6.8), 50% v/v glycerol, 25% β-  
609 mercaptoethanol, 10% SDS, 0.05% bromophenol blue) was added for analysis by SDS-  
610 PAGE and immunoblotting. Fractionation experiments were conducted at least twice for  
611 each transgenic line.

612

### 613 **Confocal Microscopy**

614 The *AtDOA10A* CDS (pDONR221) was cloned into pB7WGY2.0 to produce  
615 35S::eYFP-*AtDOA10A*, and transiently co-expressed in *Nicotiana benthamiana* epidermal  
616 cells with the ER marker VMA12-RFP (Viotti et al. 2013) via *A. tumefaciens*-mediated  
617 transformation (Kong et al. 2015). After 72 h, leaves were additionally infiltrated with 2 µg  
618 µL<sup>-1</sup> 4',6-diamidin-2-phenylindol (DAPI, Sigma-Aldrich) in ddH<sub>2</sub>O supplemented with  
619 1:20,000 v/v Triton-X (100%). Fluorescence was analyzed by confocal laser scanning  
620 microscopy using a Nikon automated Ti inverted microscope equipped with a Yokagawa  
621 CSU-X1 confocal scanning unit, a Hamamatsu C9100-02 EMCCD camera, and a Nikon S  
622 Fluor 40× numerical aperture 1.3 oil-immersion objective (Nikon). Images were taken in five

623 channels (RFP, 561/615; DAPI, 405/445nm; EYFP, 488/527nm; autofluorescence,  
624 485/705nm; and brightfield) and processed with Fiji image analysis software.

625

626

## 627 **RNA-sequencing**

628 RNA was extracted from biological triplicates of pooled 10-day old seedlings grown  
629 vertically on ½ MS plates, and samples were sequenced and analysed by Novogene UK.  
630 Briefly, mRNA was purified from total RNA using poly-T oligo-attached magnetic beads.  
631 After fragmentation, the first strand cDNA was synthesized using random hexamer primers  
632 followed by the second strand cDNA synthesis. The library was ready after end repair, A-  
633 tailing, adapter ligation, size selection, amplification, and purification. The library was  
634 checked with Qubit and real-time RT-qPCR for quantification and bioanalyzer for size  
635 distribution detection, before pooling and sequencing on Illumina platforms to generate  
636 >20M pair-end clean reads. Sequencing quality control, mapping, quantification, and  
637 differential gene expression analysis were carried out using HISAT2 software, RPKM  
638 calculations for each gene, and DESeq2 and EdgeR packages in R were used to generate  
639 lists with differentially expressed genes as described. GO enrichment analysis was carried  
640 out at geneontology.org (Ashburner et al. 2000; Mi et al. 2019).

641

## 642 **Nt-acetylome profiling**

643

644 Three biological replicates of 10-day old Arabidopsis Col-0 wild-type (WT) and  
645 *AtDOA10a/b* RNAi 4-2 seedlings (~400 mg for each sample) were processed following  
646 exactly the previously described SILProNAQ protocol (Bienvenut et al. 2017a). Following  
647 protein extraction and Bradford assay, 1mg of proteins were denatured then labelled on their  
648 N-termini and lysine ε-amino groups using N-acetoxy-[<sup>2</sup>H<sub>3</sub>] succinimide (25 μmol/mg). The  
649 labelled proteins were subjected to trypsin digestion (100 U/mg protein) and the resulting  
650 peptide mixtures were fractionated on a Strong Cation eXchange (SCX) chromatography  
651 column (Polysulfoethyl A, 200x2.1 mm, 5 μm, Hichrom, UK) to separate the acetylated N-  
652 termini and the non-acetylated internal peptides. N-termini-enriched fractions (fractions 2-11)  
653 were individually analysed by LC-MS/MS on an LTQ-Orbitrap Velos mass spectrometer.  
654 Raw data files were processed by Mascot Distiller, using the latest Araport-11 database for  
655 identification, and with mass tolerance settings of 10 ppm and 0.5 Da for the parent and  
656 fragments ions respectively. Quantification results were exported then parsed by the  
657 EnCOUNTER script (Bienvenut et al. 2017b) to obtain the datasets. Manual consolidation  
658 was then performed on all samples. This included combining the biological replicates of

659 each condition, averaging their NTA levels and the corresponding standard deviations, as  
660 well as calculating, ratios and p-values (two-tailed t-test).

661

### 662 **Cycloheximide chases and protein extractions**

663 Yeast cycloheximide (CHX) chases were performed according to the protocol  
664 described by (Buchanan et al. 2016). Transformed colonies were grown overnight in liquid  
665 DO media at 30°C before subculturing into 30ml fresh media to an OD<sub>600</sub> of 0.2. The  
666 secondary cultures were then grown at 30°C to an OD<sub>600</sub> of 1.0, then 8 ml of culture was  
667 pelleted by centrifugation before resuspending in 3.2 ml fresh 30°C DO media with 250µg  
668 ml<sup>-1</sup> CHX (in DMSO) and briefly vortexing. 950µl samples were removed at specified time  
669 points, added to 50µl of ice-cold Stop Mix (1M NaN<sub>3</sub>, 100µg ml<sup>-1</sup> BSA), centrifuged (30  
670 seconds) at 6500xg and snap-frozen. Total protein was extracted from pellets in 50µl of  
671 extraction buffer (0.1M NaOH, 50mM EDTA, 2% v/v β-mercaptoethanol, 2% v/v SDS),  
672 heated to 90°C for 20 minutes, with 0.67µl 3M acetic acid added halfway through. 12.5µl of  
673 sample buffer (250mM Tris-HCl (pH 6.8), 50% v/v glycerol, 0.05% bromophenol blue) was  
674 subsequently added. Cells were then pelleted by centrifugation and the supernatant was  
675 used for analysis.

676 Arabidopsis CHX chases were performed on seedlings grown vertically for 7 days,  
677 then transferred to liquid ½ MS for a further 3 days, at which point 300 µg ml<sup>-1</sup> CHX +/- 50  
678 µM bortezomib was added. At specified time points, 30 seedlings were blotted dry and snap-  
679 frozen. Total protein was extracted by grinding in lysis buffer (10mM Tris-HCl (pH 8.0),  
680 150mM NaCl, 0.5mM EDTA, 0.1% v/v SDS, 1% v/v Triton-X-100) with added cOmplete™,  
681 Mini, EDTA-free Protease Inhibitor Cocktail (Roche). Following pelleting of cell debris, 1/5<sup>th</sup>  
682 volume 5x sample buffer (above) was added to the supernatant prior to SDS-PAGE. All CHX  
683 chases were conducted three to four times.

684

### 685 **SDS-PAGE and Immunoblotting**

686 SDS-PAGE and immunoblotting were performed using the BIO-RAD Mini-PROTEAN  
687 system. Protein concentrations were quantified via Bradford assay, separated on 10% v/v  
688 polyacrylamide gels, transferred to a PVDF membrane, and blocked in 5% non-fat milk in  
689 TBST. Membranes were probed with primary antibodies: 1:4000 anti-β-Actin (Abcam  
690 ab184220), 1:5000 anti-β-Tubulin (Sigma-Aldrich T8328), 1:2500 anti-AtCNX1/2 (Agrisera  
691 AS12 2365), 1:4000 anti-AtUGPase (Agrisera AS05 086), 1:1000-1:3000 anti-GUS (Sigma-  
692 Aldrich G5420), 1:1000 anti-GFP/YFP (ROCHE 11814460001), 1:4000 anti-HA (Sigma-  
693 Aldrich H3663), 1:1000 anti-Myc (Antibodies.com A85281). Horseradish peroxidase-  
694 conjugated anti-mouse (Sigma-Aldrich A5278) or anti-rabbit (Cell Signalling Technology  
695 7074) secondary antibodies were subsequently added to allow development with Pierce™

696 ECL Western Blotting Substrate (ThermoFisher Scientific) and ECL Hyperfilm film  
697 (Amersham). Band densities were quantified relative to the most intense band following  
698 normalisation to actin/tubulin using Fiji image analysis software. All stability assays were  
699 conducted at least three times.

700

#### 701 **Accession Numbers**

702 RNA-seq data are available at the NCBI GEO database with accession codes GSE236282  
703 (for *doa10a/b RNAi 4-2* and its related Col-0 WT, *amiNAA10*, and *Atnaa20* data sets) and  
704 GSE161571 (for Col-0 WT datasets related to *amiNAA10* and *Atnaa20* analyses). Nt-  
705 acetylome data are available at the Proteomics Identification Database (PRIDE) with  
706 accession code PXD043217.

707

708

709

710

711

712

713

714

715

716

717

718

719

720

721

722

723

724

725

726

727

728

729

730

#### 731 **Funding information**

732 D.J.G, R.D.E and M.B were funded by a Biotechnology and Biological Sciences Research  
 733 Council grant (BB/M020568/1) and European Research Council Starting Grant (ERC-StG  
 734 715441-GasPlaNt). Research in Heidelberg was performed within projects (IDs: 353859218  
 735 and 496871662) granted to M.W. (WI 3560/4-1 and 7-1). Research in CG team was  
 736 supported by KatNat (ERA-NET, ANR-17-CAPS-0001-01) and CanMore (France-Germany  
 737 PRCI, ANR-20 CE92-0040), and SPS ANR-17-EUR-0007, EUR SPS-GSR, ANR-11-IDEX-  
 738 0003-02.X.C was funded by a China Scholarship Council PhD studentship.

739

#### 740 **Acknowledgments**

741 This work has benefited from facilities and expertise of the I2BC proteomic platform  
 742 supported by IBSA, Ile de France Region, Plan Cancer, CNRS and Paris-Sud University.  
 743 We would also like to thank the Nikon Imaging Center at the University of Heidelberg.

744

#### 745 **Author contributions**

746

747 D.J.G, R.D.E and M.B conceived and designed the study. R.D.E, M.B, J.B.B, L.A, X.C,  
 748 J.C.C, T.M, M.W, C.G and D.J.G performed research and analysed data. D.J.G and R.D.E  
 749 wrote the manuscript. All authors revised and approved the article.

750

#### 751 **Figure Legends**

752

753 **Figure 1. Structure, functional conservation and phylogeny of Arabidopsis DOA10-**  
 754 **like proteins.** (A) Schematic diagram of Arabidopsis (At) DOA10 proteins compared to the  
 755 single yeast (Sc) homolog. Key domains and features are shown. (B) Percentage identity  
 756 between Arabidopsis and yeast DOA10 proteins. Values are shown for total protein length,  
 757 and the RING-CH and TD regions. See also Figure S1. (C) Transgene-specific RT-PCR  
 758 (using 5' and 3' primer pairs) confirming *AtDOA10A/B-GFP* expression in *Scdoa10Δ* mutant  
 759 yeast cells. (D) The *Scdoa10Δ* yeast mutant is insensitive to hygromycin relative to WT cells.  
 760 *AtDOA10A-GFP* can complement this phenotype, whereas *AtDOA10B-GFP* cannot. Spots  
 761 represent 10-fold dilutions from left to right. (E) Inferred phylogenetic tree of full-length  
 762 DOA10-like protein homologs identified in various diploid angiosperm species, yeast and  
 763 human (*HsMARCH6*). Two main groups are identified: (i) a DOA10A-like clade, which is  
 764 split between monocot and dicot lineages, and (ii) a DOA10B-like clade that is comprised of  
 765 Brassicaceae-derived sequences only. Bootstrap values are shown and the separate  
 766 Brassicaceae groupings are highlighted with a blue box. At, *Arabidopsis thaliana*; Al,  
 767 *Arabidopsis lyrata*; Br, *Brassica rapa*; Cr, *Capsella rubella*; Os, *Oryza sativa*; Bd,  
 768 *Brachypodium distachyon*; Ac, *Ananas comosus*; Sl, *Solanum lycopersicum*; Ca, *Capsicum*

769 *anuum*; Gm, *Glycine max*; Mt, *Medicago truncatula*; Pt, *Populus trichocarpa*; Rc, *Ricinus*  
770 *communis*. Tree not drawn to scale.

771

772 **Figure 2. AtDOA10A and AtDOA10B are broadly expressed in seedlings and localise**  
773 **to the endoplasmic reticulum.** (A) Histochemical staining of 7- and 14-day old Arabidopsis  
774 seedlings expressing *pDOA10A/B::AtDOA10A/B-GUS*. Scale bar for all images: 1mm. (B)  
775 RT-qPCR of endogenous *AtDOA10A* and *B* mRNA in different seedlings and adult tissues  
776 (note the Y-axis Log<sub>10</sub> scale). Relative expression levels were calculated through  
777 normalisation to *AtACT7* and are the average of three biological repeats. Horizontal line  
778 shows mean. (C) anti-GUS immunoblot of microsomal and soluble protein extracts from  
779 seedlings expressing *pDOA10A/B::AtDOA10A/B-GUS* (expected sizes: *AtDOA10A-GUS*,  
780 ~195 kDa; *AtDOA10B-GUS*, ~170kDa – although both are detected at around 250 kDa).  
781 Anti-CNX1/2 (microsomal) and anti-UGPase (soluble) control blots confirming efficacy of the  
782 fractionation are shown. (D) Confocal images of *N. benthamiana* leaf pavement cells  
783 transiently co-expressing eYFP-*AtDOA10A* and the ER-marker protein *AtVMA12-RFP*  
784 showing co-localisation of YFP and RFP signals. Nuclei are stained with DAPI, and  
785 chloroplast auto-fluorescence is also shown. Scale bar: 10µm.

786

787 **Figure 3. Generation and phenotypic assessment of AtDOA10A and B mutants.** (A)  
788 Schematic of *AtDOA10A* and *B* genes, showing 5'/3' UTR (black) and exons (grey), T-DNA  
789 IDs and insertion sites, position of RNAi construct sequences and RT-qPCR primers used in  
790 (B). (B) RT-qPCR of endogenous *AtDOA10B* in the *Atdoa10A* control line and homozygous  
791 RNAi lines 3-7 and 4-2, using primer pairs (P1 and P2) upstream and downstream of the  
792 RNAi target sequence. Expression levels were normalised to *AtACT7* and expression in the  
793 RNAi lines is shown relative to the endogenous levels of *DOA10B* in the untransformed  
794 *Atdoa10A* mutant. Data are the average of three biological repeats. Horizontal line shows  
795 the mean. (C) Rosettes of 6-week-old WT, *Atdoa10a*, *Atdoa10b* and *Atdoa10a/b RNAi 4-2*  
796 lines grown under short days. Images were digitally extracted for comparison. Scale bar:  
797 2cm (D) 7- and 14-day old seedlings grown on control or 0.5µM ABA-supplemented ½ MS  
798 plates. Scale bar: 5mm.

799

800 **Figure 4. RNA-seq and Nt-acetylome profiling indicate that AtDOA10s do not regulate**  
801 **global turnover of Nt-acetylated proteins.** (A) Volcano plot of Up and Down DEGs in 10-  
802 day old seedlings of *Atdoa10a/b RNAi 4-2* vs Col-0. Orange data points represent mRNAs  
803 that are >2-fold up or down (log<sub>10</sub>(q)>5). (B) Venn diagram showing overlap in total DEGs  
804 (excluding non-annotated mRNAs) relative to Col-0 between 10-day old seedlings of  
805 *Atdoa10a/b RNAi 4-2*, *amiNAA10* and *naa20*. (C) Summary table of N-terminal profiling. (D)

806 Venn diagrams showing numbers and overlap of (i) identified N-termini and (ii) quantified N-  
 807 termini in *Atdoa10a/b RNAi 4-2* vs Col-0. (E) Global NTA variations comparison in  
 808 *Adoa10a/b RNAi 4-2* and Col-0. For each sample, the peptides were sorted in decreasing  
 809 order of %NTA (quantitated only). Each Nt-peptide was assigned a number corresponding to  
 810 its relative position. These protein numbers are plotted with matching NTA yield (%), either  
 811 for all Nt-acetylation positions, protein Nt-positions (pos. 1 or 2), or downstream Nt-  
 812 acetylation (pos. >2) (F) Relative abundance of acetylated Nt-residues (shown as %) in  
 813 *Atdoa10a/b RNAi 4-2* and Col-0. (G) Relative comparison of NTA levels between  
 814 *Atdoa10a/b RNAi 4-2* and Col-0, for peptides quantified in both datasets, showed no  
 815 significant ( $p < 0.05$ ) differences.

816

817 **Figure 5. Proteolytic turnover of AtSQE1 by AtDOA10A and AtNAA20 in heterologous**  
 818 **yeast degradation assays.** (A) Anti-HA immunoblot showing steady state levels of

819 AtSQE1-HA in WT vs *Scdoa10Δ* yeast cells. Anti-ACTIN bands are shown on the same blot.  
 820 CBB: coomassie brilliant blue loading control. (B) Steady-state protein (immunoblot) and  
 821 mRNA (RT-PCR) levels of AtSQE1-HA expressed in WT vs *Scdoa10Δ* +/- co-expression  
 822 with AtDOA10A or AtDOA10B. (C) Cycloheximide (CHX) chase of AtSQE1-HA in WT,  
 823 *Scdoa10Δ* and *Scnaa20Δ* yeast cells (immunoblot and quantified relative density). (D)  
 824 Cycloheximide chase showing that co-expression of AtDOA10A destabilises AtSQE1-HA in  
 825 *Scdoa10Δ* yeast cells (immunoblot and quantified relative density). (E) Cycloheximide chase  
 826 showing that co-expression of AtNAA20 destabilises AtSQE1-HA in *Scnaa20Δ* yeast cells  
 827 (immunoblot and quantified relative density).

828

829 **Figure 6. Impact of N-terminal mutagenesis on AtSQE1 stability suggests indirect**

830 **effects of Nt-acetyltransferases on protein turnover in yeast.** (A) Summary of N-terminal

831 (Nt) mutants and predicted respective NAT activities. (B) Steady-state protein levels of  
 832 AtSQE1-HA Nt-variants in WT and *Scdoa10Δ* yeast cells (C) Cycloheximide (CHX) chase of  
 833 WT ME- and mutant MP-AtSQE1-HA in WT yeast cells (immunoblot and quantified relative  
 834 density). (D) Cycloheximide (CHX) chase of WT ME-AtSQE1-HA in WT and *Scnaa10Δ* yeast  
 835 cells (immunoblot and quantified relative density). (E) Cycloheximide (CHX) chase of mutant  
 836 MA-AtSQE1-HA in WT and *Scnaa20Δ* yeast cells (immunoblot and quantified relative  
 837 density). (F) Cycloheximide (CHX) chase of mutant MA-AtSQE1-HA in WT and *Scnaa10Δ*  
 838 yeast cells (immunoblot and quantified relative density).

839

840 **Figure 7. Nt-acetylation-independent turnover of AtSQE1 by AtDOA10 in Arabidopsis.**

841 (A) Microsomal and soluble protein extracts from seedlings expressing WT ME- and mutant  
 842 MP-AtSQE1-Myc. Anti-CNX1/2 (microsomal) and anti-UGPase (soluble) control blots



843 confirming efficacy of the fractionation are shown. (B) Cycloheximide (CHX) chase of WT  
 844 ME- and mutant MP-AtSQE1-Myc variants in WT Col-0 and different mutant backgrounds.  
 845 Independent transgenics have different starting expression levels (see Fig. S6A) and so  
 846 comparisons of protein levels can only be directly made between time points within lines. (C)  
 847 Cycloheximide (CHX) chase of WT ME-AtSQE1-HA in Col-0 and *Atdoa10a/b RNAi 4-2*  
 848 seedlings (immunoblot and quantified relative density). (D) 7-day old seedlings on ½ MS  
 849 showing epinasty in *Atdoa10a/b RNAi 4-2*. scale bar: 5mm. (E) LDAO chase of WT ME-  
 850 AtSQE1-Myc in Col-0 and *Atdoa10a/b RNAi 4-2* seedlings (immunoblot and quantified  
 851 relative density). (F) Terbinafine chase of WT ME-AtSQE1-Myc in Col-0.

852

853 **Figure 8. Summary of the mevalonate (MVA) and sterol synthesis pathways in**  
 854 **Arabidopsis:** (1) DOA10 negatively regulates SQE1 stability (this study) and positively  
 855 regulates HMGR activity (Doblas *et al.* 2013) in plants, yeast and humans. Yeast and animal  
 856 SQEs were previously shown to be targets of DOA10 (Foresti *et al.* 2013; Zelcer *et al.*  
 857 2014), indicating conservation of this regulatory module across three eukaryotic kingdoms.  
 858 (2) NATA and B were shown to indirectly contribute to AtSQE1 turnover in yeast (this study),  
 859 but not in Arabidopsis. (3) LDAO, an inhibitor of several downstream enzymatic steps, also  
 860 negatively regulates AtSQE1 levels via DOA10-independent mechanism(s). (4) Terbinafine,  
 861 a chemical inhibitor of SQE enzymatic activity (Nowosielski *et al.*, 2011), indirectly promotes  
 862 accumulation of AtSQE1 (this study), likely through positive feedback. Dashed lines denote  
 863 indirect effects.

864

## 865 References

866

- 867 Aksnes H, Drazic A, Marie M, Arnesen T (2016) First Things First: Vital Protein Marks by N-  
 868 Terminal Acetyltransferases. *Trends Biochem Sci* 41 (9):746-760.  
 869 doi:10.1016/j.tibs.2016.07.005
- 870 Aksnes H, Goris M, Stromland O, Drazic A, Waheed Q, Reuter N, Arnesen T (2017) Molecular  
 871 determinants of the N-terminal acetyltransferase Naa60 anchoring to the Golgi  
 872 membrane. *J Biol Chem* 292 (16):6821-6837. doi:10.1074/jbc.M116.770362
- 873 Aksnes H, Ree R, Arnesen T (2019) Co-translational, Post-translational, and Non-catalytic  
 874 Roles of N-Terminal Acetyltransferases. *Mol Cell* 73 (6):1097-1114.  
 875 doi:10.1016/j.molcel.2019.02.007
- 876 Aksnes H, Van Damme P, Goris M, Starheim KK, Marie M, Stove SI, Hoel C, Kalvik TV, Hole K,  
 877 Glomnes N, *et al.* (2015) An organellar alpha-acetyltransferase, *naa60*, acetylates  
 878 cytosolic N termini of transmembrane proteins and maintains Golgi integrity. *Cell*  
 879 *Rep* 10 (8):1362-1374. doi:10.1016/j.celrep.2015.01.053
- 880 Arnesen T, Van Damme P, Polevoda B, Helsens K, Evjenth R, Colaert N, Varhaug JE,  
 881 Vandekerckhove J, Lillehaug JR, Sherman F, *et al.* (2009) Proteomics analyses reveal  
 882 the evolutionary conservation and divergence of N-terminal acetyltransferases from

- 883 yeast and humans. *Proc Natl Acad Sci U S A* 106 (20):8157-8162.  
884 doi:10.1073/pnas.0901931106
- 885 Ashburner M, Ball CA, Blake JA, Botstein D, Butler H, Cherry JM, Davis AP, Dolinski K, Dwight  
886 SS, Eppig JT, et al. (2000) Gene ontology: tool for the unification of biology. The Gene  
887 Ontology Consortium. *Nat Genet* 25 (1):25-29. doi:10.1038/75556
- 888 Bienvenut WV, Brunje A, Boyer JB, Muhlenbeck JS, Bernal G, Lassowskat I, Dian C, Linster E,  
889 Dinh TV, Koskela MM, et al. (2020) Dual lysine and N-terminal acetyltransferases  
890 reveal the complexity underpinning protein acetylation. *Mol Syst Biol* 16 (7):e9464.  
891 doi:10.15252/msb.20209464
- 892 Bienvenut WV, Giglione C, Meinnel T (2017a) SILProNAQ: A Convenient Approach for  
893 Proteome-Wide Analysis of Protein N-Termini and N-Terminal Acetylation  
894 Quantitation. *Methods Mol Biol* 1574:17-34. doi:10.1007/978-1-4939-6850-3\_3
- 895 Bienvenut WV, Scarpelli JP, Dumestier J, Meinnel T, Giglione C (2017b) EnCOUNTER: a  
896 parsing tool to uncover the mature N-terminus of organelle-targeted proteins in  
897 complex samples. *BMC Bioinformatics* 18 (1):182. doi:10.1186/s12859-017-1595-y
- 898 Bienvenut WV, Sumpton D, Martinez A, Lilla S, Espagne C, Meinnel T, Giglione C (2012)  
899 Comparative large scale characterization of plant versus mammal proteins reveals  
900 similar and idiosyncratic N-alpha-acetylation features. *Mol Cell Proteomics* 11  
901 (6):M111 015131. doi:10.1074/mcp.M111.015131
- 902 Buchanan BW, Lloyd ME, Engle SM, Rubenstein EM (2016) Cycloheximide Chase Analysis of  
903 Protein Degradation in *Saccharomyces cerevisiae*. *J Vis Exp* (110). doi:10.3791/53975
- 904 Carland F, Fujioka S, Nelson T (2010) The sterol methyltransferases SMT1, SMT2, and SMT3  
905 influence *Arabidopsis* development through nonbrassinosteroid products. *Plant*  
906 *Physiol* 153 (2):741-756. doi:10.1104/pp.109.152587
- 907 Cui F, Liu L, Zhao Q, Zhang Z, Li Q, Lin B, Wu Y, Tang S, Xie Q (2012) *Arabidopsis* ubiquitin  
908 conjugase UBC32 is an ERAD component that functions in brassinosteroid-mediated  
909 salt stress tolerance. *Plant Cell* 24 (1):233-244. doi:10.1105/tpc.111.093062
- 910 Darnet S, Martin LBB, Mercier P, Bracher F, Geoffroy P, Schaller H (2020) Inhibition of  
911 Phytosterol Biosynthesis by Azasterols. *Molecules* 25 (5).  
912 doi:10.3390/molecules25051111
- 913 De Vriese K, Pollier J, Goossens A, Beeckman T, Vanneste S (2021) Dissecting cholesterol and  
914 phytosterol biosynthesis via mutants and inhibitors. *J Exp Bot* 72 (2):241-253.  
915 doi:10.1093/jxb/eraa429
- 916 Dinh TV, Bienvenut WV, Linster E, Feldman-Salit A, Jung VA, Meinnel T, Hell R, Giglione C,  
917 Wirtz M (2015) Molecular identification and functional characterization of the first  
918 N-alpha-acetyltransferase in plastids by global acetylome profiling. *Proteomics* 15  
919 (14):2426-2435. doi:10.1002/pmic.201500025
- 920 Doblas VG, Amorim-Silva V, Pose D, Rosado A, Esteban A, Arro M, Azevedo H, Bombarely A,  
921 Borsani O, Valpuesta V, et al. (2013) The SUD1 gene encodes a putative E3 ubiquitin  
922 ligase and is a positive regulator of 3-hydroxy-3-methylglutaryl coenzyme a  
923 reductase activity in *Arabidopsis*. *Plant Cell* 25 (2):728-743.  
924 doi:10.1105/tpc.112.108696
- 925 Drazic A, Aksnes H, Marie M, Boczkowska M, Varland S, Timmerman E, Foyn H, Glomnes N,  
926 Rebowski G, Impens F, et al. (2018) NAA80 is actin's N-terminal acetyltransferase and  
927 regulates cytoskeleton assembly and cell motility. *Proc Natl Acad Sci U S A* 115  
928 (17):4399-4404. doi:10.1073/pnas.1718336115

- 929 Foresti O, Ruggiano A, Hannibal-Bach HK, Ejsing CS, Carvalho P (2013) Sterol homeostasis  
930 requires regulated degradation of squalene monooxygenase by the ubiquitin ligase  
931 Doa10/Teb4. *Elife* 2:e00953. doi:10.7554/eLife.00953
- 932 Friedrich UA, Zedan M, Hessling B, Fenzl K, Gillet L, Barry J, Knop M, Kramer G, Bukau B  
933 (2021) N(alpha)-terminal acetylation of proteins by NatA and NatB serves distinct  
934 physiological roles in *Saccharomyces cerevisiae*. *Cell Rep* 34 (5):108711.  
935 doi:10.1016/j.celrep.2021.108711
- 936 Gibbs DJ (2015) Emerging Functions for N-Terminal Protein Acetylation in Plants. *Trends*  
937 *Plant Sci* 20 (10):599-601. doi:10.1016/j.tplants.2015.08.008
- 938 Gibbs DJ, Bailey M, Etherington RD (2022) A stable start: cotranslational Nt-acetylation  
939 promotes proteome stability across kingdoms. *Trends Cell Biol.*  
940 doi:10.1016/j.tcb.2022.02.004
- 941 Gibbs DJ, Bailey M, Tedds HM, Holdsworth MJ (2016) From start to finish: amino-terminal  
942 protein modifications as degradation signals in plants. *New Phytol* 211 (4):1188-  
943 1194. doi:10.1111/nph.14105
- 944 Giglione C, Meinel T (2021) Evolution-Driven Versatility of N Terminal Acetylation in  
945 Photoautotrophs. *Trends Plant Sci* 26 (4):375-391. doi:10.1016/j.tplants.2020.11.012
- 946 Gill S, Stevenson J, Kristiana I, Brown AJ (2011) Cholesterol-dependent degradation of  
947 squalene monooxygenase, a control point in cholesterol synthesis beyond HMG-CoA  
948 reductase. *Cell Metab* 13 (3):260-273. doi:10.1016/j.cmet.2011.01.015
- 949 Goetze S, Qeli E, Mosimann C, Staes A, Gerrits B, Roschitzki B, Mohanty S, Niederer EM,  
950 Laczko E, Timmerman E, et al. (2009) Identification and functional characterization of  
951 N-terminally acetylated proteins in *Drosophila melanogaster*. *PLoS Biol* 7  
952 (11):e1000236. doi:10.1371/journal.pbio.1000236
- 953 Gong X, Huang Y, Liang Y, Yuan Y, Liu Y, Han T, Li S, Gao H, Lv B, Huang X, et al. (2022)  
954 OsHYPK-mediated protein N-terminal acetylation coordinates plant development  
955 and abiotic stress responses in rice. *Mol Plant* 15 (4):740-754.  
956 doi:10.1016/j.molp.2022.03.001
- 957 Gouy M, Tannier E, Comte N, Parsons DP (2021) Seaview Version 5: A Multiplatform  
958 Software for Multiple Sequence Alignment, Molecular Phylogenetic Analyses, and  
959 Tree Reconciliation. *Methods Mol Biol* 2231:241-260. doi:10.1007/978-1-0716-1036-  
960 7\_15
- 961 Habeck G, Ebner FA, Shimada-Kreft H, Kreft SG (2015) The yeast ERAD-C ubiquitin ligase  
962 Doa10 recognizes an intramembrane degron. *J Cell Biol* 209 (2):261-273.  
963 doi:10.1083/jcb.201408088
- 964 Hershko A, Heller H, Eytan E, Kaklij G, Rose IA (1984) Role of the alpha-amino group of  
965 protein in ubiquitin-mediated protein breakdown. *Proc Natl Acad Sci U S A* 81  
966 (22):7021-7025. doi:10.1073/pnas.81.22.7021
- 967 Hirsch C, Gauss R, Horn SC, Neuber O, Sommer T (2009) The ubiquitylation machinery of the  
968 endoplasmic reticulum. *Nature* 458 (7237):453-460. doi:10.1038/nature07962
- 969 Huber M, Armbruster L, Etherington RD, De La Torre C, Hawkesford MJ, Sticht C, Gibbs DJ,  
970 Hell R, Wirtz M (2021) Disruption of the N(alpha)-Acetyltransferase NatB Causes  
971 Sensitivity to Reductive Stress in *Arabidopsis thaliana*. *Front Plant Sci* 12:799954.  
972 doi:10.3389/fpls.2021.799954
- 973 Huber M, Bienvenut WV, Linster E, Stephan I, Armbruster L, Sticht C, Layer D, Lapouge K,  
974 Meinel T, Sinning I, et al. (2020) NatB-Mediated N-Terminal Acetylation Affects

975 Growth and Biotic Stress Responses. *Plant Physiol* 182 (2):792-806.  
 976 doi:10.1104/pp.19.00792

977 Hwang CS, Shemorry A, Varshavsky A (2010) N-terminal acetylation of cellular proteins  
 978 creates specific degradation signals. *Science* 327 (5968):973-977.  
 979 doi:10.1126/science.1183147

980 Karimi M, Inze D, Depicker A (2002) GATEWAY vectors for Agrobacterium-mediated plant  
 981 transformation. *Trends Plant Sci* 7 (5):193-195. doi:10.1016/s1360-1385(02)02251-3

982 Kats I, Khmelinskii A, Kschonsak M, Huber F, Knieß RA, Bartosik A, Knop M (2018) Mapping  
 983 Degradation Signals and Pathways in a Eukaryotic N-terminome. *Molecular Cell* 70  
 984 (3):488-501.e485. doi:10.1016/j.molcel.2018.03.033

985 Kim HK, Kim RR, Oh JH, Cho H, Varshavsky A, Hwang CS (2014) The N-terminal methionine of  
 986 cellular proteins as a degradation signal. *Cell* 156 (1-2):158-169.  
 987 doi:10.1016/j.cell.2013.11.031

988 Kim JH, Cho SK, Oh TR, Ryu MY, Yang SW, Kim WT (2017) MPSR1 is a cytoplasmic PQC E3  
 989 ligase for eliminating emergent misfolded proteins in *Arabidopsis thaliana*. *Proc Natl*  
 990 *Acad Sci U S A* 114 (46):E10009-E10017. doi:10.1073/pnas.1713574114

991 Kong L, Cheng J, Zhu Y, Ding Y, Meng J, Chen Z, Xie Q, Guo Y, Li J, Yang S, et al. (2015)  
 992 Degradation of the ABA co-receptor ABI1 by PUB12/13 U-box E3 ligases. *Nat*  
 993 *Commun* 6:8630. doi:10.1038/ncomms9630

994 Koskela MM, Brunje A, Ivanauskaite A, Grabsztunowicz M, Lassowskat I, Neumann U, Dinh  
 995 TV, Sindlinger J, Schwarzer D, Wirtz M, et al. (2018) Chloroplast Acetyltransferase  
 996 NSI Is Required for State Transitions in *Arabidopsis thaliana*. *Plant Cell* 30 (8):1695-  
 997 1709. doi:10.1105/tpc.18.00155

998 Kozak M (1997) Recognition of AUG and alternative initiator codons is augmented by G in  
 999 position +4 but is not generally affected by the nucleotides in positions +5 and +6.  
 1000 *EMBO J* 16 (9):2482-2492. doi:10.1093/emboj/16.9.2482

1001 Kreft SG, Hochstrasser M (2011) An unusual transmembrane helix in the endoplasmic  
 1002 reticulum ubiquitin ligase Doa10 modulates degradation of its cognate E2 enzyme. *J*  
 1003 *Biol Chem* 286 (23):20163-20174. doi:10.1074/jbc.M110.196360

1004 Kreft SG, Wang L, Hochstrasser M (2006) Membrane topology of the yeast endoplasmic  
 1005 reticulum-localized ubiquitin ligase Doa10 and comparison with its human ortholog  
 1006 TEB4 (MARCH-VI). *J Biol Chem* 281 (8):4646-4653. doi:10.1074/jbc.M512215200

1007 Laranjeira S, Amorim-Silva V, Esteban A, Arro M, Ferrer A, Tavares RM, Botella MA, Rosado  
 1008 A, Azevedo H (2015) *Arabidopsis* Squalene Epoxidase 3 (SQE3) Complements SQE1  
 1009 and Is Important for Embryo Development and Bulk Squalene Epoxidase Activity.  
 1010 *Mol Plant* 8 (7):1090-1102. doi:10.1016/j.molp.2015.02.007

1011 Leber R, Zenz R, Schrottner K, Fuchsbichler S, Puhringer B, Turnowsky F (2001) A novel  
 1012 sequence element is involved in the transcriptional regulation of expression of the  
 1013 ERG1 (squalene epoxidase) gene in *Saccharomyces cerevisiae*. *Eur J Biochem* 268  
 1014 (4):914-924. doi:10.1046/j.1432-1327.2001.01940.x

1015 Li LM, Lu SY, Li RJ (2017) The *Arabidopsis* endoplasmic reticulum associated degradation  
 1016 pathways are involved in the regulation of heat stress response. *Biochem Biophys*  
 1017 *Res Commun* 487 (2):362-367. doi:10.1016/j.bbrc.2017.04.066

1018 Li Z, Dogra V, Lee KP, Li R, Li M, Li M, Kim C (2020) N-Terminal Acetylation Stabilizes SIGMA  
 1019 FACTOR BINDING PROTEIN1 Involved in Salicylic Acid-Primed Cell Death. *Plant*  
 1020 *Physiol* 183 (1):358-370. doi:10.1104/pp.19.01417

- 1021 Linster E, Forero Ruiz FL, Miklankova P, Ruppert T, Mueller J, Armbruster L, Gong X, Serino  
1022 G, Mann M, Hell R, et al. (2022) Cotranslational N-degron masking by acetylation  
1023 promotes proteome stability in plants. *Nature Communications* 13 (1):810.  
1024 doi:10.1038/s41467-022-28414-5
- 1025 Linster E, Layer D, Bienvenut WV, Dinh TV, Weyer FA, Leemhuis W, Brunje A, Hoffrichter M,  
1026 Miklankova P, Kopp J, et al. (2020) The Arabidopsis N(alpha) -acetyltransferase  
1027 NAA60 locates to the plasma membrane and is vital for the high salt stress response.  
1028 *New Phytol* 228 (2):554-569. doi:10.1111/nph.16747
- 1029 Linster E, Stephan I, Bienvenut WV, Maple-Grodem J, Myklebust LM, Huber M, Reichelt M,  
1030 Sticht C, Moller SG, Meinnel T, et al. (2015) Downregulation of N-terminal  
1031 acetylation triggers ABA-mediated drought responses in Arabidopsis. *Nat Commun*  
1032 6:7640. doi:10.1038/ncomms8640
- 1033 Linster E, Wirtz M (2018) N-terminal acetylation: an essential protein modification emerges  
1034 as an important regulator of stress responses. *J Exp Bot* 69 (19):4555-4568.  
1035 doi:10.1093/jxb/ery241
- 1036 Liu L, Cui F, Li Q, Yin B, Zhang H, Lin B, Wu Y, Xia R, Tang S, Xie Q (2011) The endoplasmic  
1037 reticulum-associated degradation is necessary for plant salt tolerance. *Cell Res* 21  
1038 (6):957-969. doi:10.1038/cr.2010.181
- 1039 Livak KJ, Schmittgen TD (2001) Analysis of Relative Gene Expression Data Using Real-Time  
1040 Quantitative PCR and the 2- $\Delta\Delta$ CT Method. *Methods* 25 (4):402-408.  
1041 doi:<https://doi.org/10.1006/meth.2001.1262>
- 1042 Lu S, Zhao H, Des Marais DL, Parsons EP, Wen X, Xu X, Bangarusamy DK, Wang G, Rowland  
1043 O, Juenger T, et al. (2012) Arabidopsis ECERIFERUM9 involvement in cuticle  
1044 formation and maintenance of plant water status. *Plant Physiol* 159 (3):930-944.  
1045 doi:10.1104/pp.112.198697
- 1046 Mi H, Muruganujan A, Ebert D, Huang X, Thomas PD (2019) PANTHER version 14: more  
1047 genomes, a new PANTHER GO-slim and improvements in enrichment analysis tools.  
1048 *Nucleic Acids Res* 47 (D1):D419-D426. doi:10.1093/nar/gky1038
- 1049 Mueller F, Friese A, Pathe C, da Silva RC, Rodriguez KB, Musacchio A, Bange T (2021) Overlap  
1050 of NatA and IAP substrates implicates N-terminal acetylation in protein stabilization.  
1051 *Sci Adv* 7 (3). doi:10.1126/sciadv.abc8590
- 1052 Nakagawa T, Suzuki T, Murata S, Nakamura S, Hino T, Maeo K, Tabata R, Kawai T, Tanaka K,  
1053 Niwa Y, et al. (2007) Improved Gateway binary vectors: high-performance vectors for  
1054 creation of fusion constructs in transgenic analysis of plants. *Biosci Biotechnol*  
1055 *Biochem* 71 (8):2095-2100. doi:10.1271/bbb.70216
- 1056 Nguyen KT, Lee CS, Mun SH, Truong NT, Park SK, Hwang CS (2019) N-terminal acetylation  
1057 and the N-end rule pathway control degradation of the lipid droplet protein PLIN2. *J*  
1058 *Biol Chem* 294 (1):379-388. doi:10.1074/jbc.RA118.005556
- 1059 Nowosielski M, Hoffmann M, Wyrwicz LS, Stepniak P, Plewczynski DM, Lazniewski M,  
1060 Ginalski K, Rychlewski L (2011) Detailed mechanism of squalene epoxidase inhibition  
1061 by terbinafine. *J Chem Inf Model* 51 (2):455-462. doi:10.1021/ci100403b
- 1062 Park SE, Kim JM, Seok OH, Cho H, Wadas B, Kim SY, Varshavsky A, Hwang CS (2015) Control  
1063 of mammalian G protein signaling by N-terminal acetylation and the N-end rule  
1064 pathway. *Science* 347 (6227):1249-1252. doi:10.1126/science.aaa3844
- 1065 Rasbery JM, Shan H, LeClair RJ, Norman M, Matsuda SP, Bartel B (2007) Arabidopsis thaliana  
1066 squalene epoxidase 1 is essential for root and seed development. *J Biol Chem* 282  
1067 (23):17002-17013. doi:10.1074/jbc.M611831200

1068 Ravid T, Kreft SG, Hochstrasser M (2006) Membrane and soluble substrates of the Doa10  
1069 ubiquitin ligase are degraded by distinct pathways. *EMBO J* 25 (3):533-543.  
1070 doi:10.1038/sj.emboj.7600946

1071 Ree R, Varland S, Arnesen T (2018) Spotlight on protein N-terminal acetylation. *Exp Mol*  
1072 *Med* 50 (7):1-13. doi:10.1038/s12276-018-0116-z

1073 Schmidt CC, Vasic V, Stein A (2020) Doa10 is a membrane protein retrotranslocase in ER-  
1074 associated protein degradation. *Elife* 9. doi:10.7554/eLife.56945

1075 Scott NA, Sharpe LJ, Capell-Hattam IM, Gullo SJ, Luu W, Brown AJ (2020) The cholesterol  
1076 synthesis enzyme lanosterol 14 $\alpha$ -demethylase is post-translationally regulated  
1077 by the E3 ubiquitin ligase MARCH6. *Biochem J* 477 (2):541-555.  
1078 doi:10.1042/BCJ20190647

1079 Sharpe LJ, Coates HW, Brown AJ (2020) Post-translational control of the long and winding  
1080 road to cholesterol. *J Biol Chem* 295 (51):17549-17559.  
1081 doi:10.1074/jbc.REV120.010723

1082 Shemorry A, Hwang CS, Varshavsky A (2013) Control of protein quality and stoichiometries  
1083 by N-terminal acetylation and the N-end rule pathway. *Mol Cell* 50 (4):540-551.  
1084 doi:10.1016/j.molcel.2013.03.018

1085 Starheim KK, Gevaert K, Arnesen T (2012) Protein N-terminal acetyltransferases: when the  
1086 start matters. *Trends Biochem Sci* 37 (4):152-161. doi:10.1016/j.tibs.2012.02.003

1087 Strasser R (2018) Protein Quality Control in the Endoplasmic Reticulum of Plants. *Annu Rev*  
1088 *Plant Biol* 69:147-172. doi:10.1146/annurev-arplant-042817-040331

1089 Swanson R, Locher M, Hochstrasser M (2001) A conserved ubiquitin ligase of the nuclear  
1090 envelope/endoplasmic reticulum that functions in both ER-associated and  
1091 Matalpha2 repressor degradation. *Genes Dev* 15 (20):2660-2674.  
1092 doi:10.1101/gad.933301

1093 Viotti C, Kruger F, Krebs M, Neubert C, Fink F, Lupanga U, Scheuring D, Boutte Y, Frescatada-  
1094 Rosa M, Wolfenstetter S, et al. (2013) The endoplasmic reticulum is the main  
1095 membrane source for biogenesis of the lytic vacuole in Arabidopsis. *Plant Cell* 25  
1096 (9):3434-3449. doi:10.1105/tpc.113.114827

1097 Wiame E, Tahay G, Tyteca D, Vertommen D, Stroobant V, Bommer GT, Van Schaftingen E  
1098 (2018) NAT6 acetylates the N-terminus of different forms of actin. *FEBS J* 285  
1099 (17):3299-3316. doi:10.1111/febs.14605

1100 Xu F, Huang Y, Li L, Gannon P, Linster E, Huber M, Kapos P, Bienvenut W, Polevoda B,  
1101 Meinnel T, et al. (2015) Two N-terminal acetyltransferases antagonistically regulate  
1102 the stability of a nod-like receptor in Arabidopsis. *Plant Cell* 27 (5):1547-1562.  
1103 doi:10.1105/tpc.15.00173

1104 Zelcer N, Sharpe LJ, Loregger A, Kristiana I, Cook EC, Phan L, Stevenson J, Brown AJ (2014)  
1105 The E3 ubiquitin ligase MARCH6 degrades squalene monooxygenase and affects 3-  
1106 hydroxy-3-methyl-glutaryl coenzyme A reductase and the cholesterol synthesis  
1107 pathway. *Mol Cell Biol* 34 (7):1262-1270. doi:10.1128/MCB.01140-13

1108 Zhang X, Henriques R, Lin SS, Niu QW, Chua NH (2006) Agrobacterium-mediated  
1109 transformation of Arabidopsis thaliana using the floral dip method. *Nat Protoc* 1  
1110 (2):641-646. doi:10.1038/nprot.2006.97

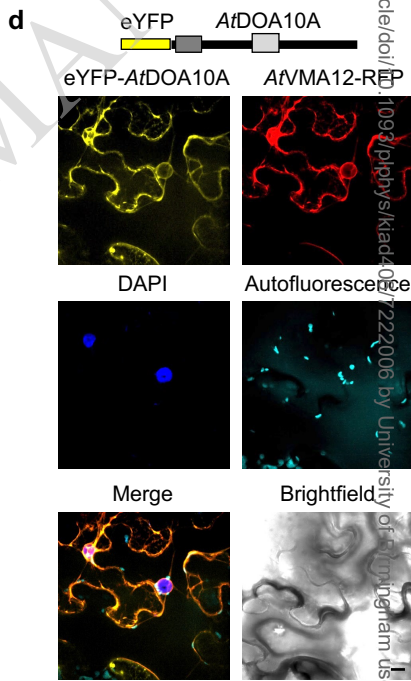
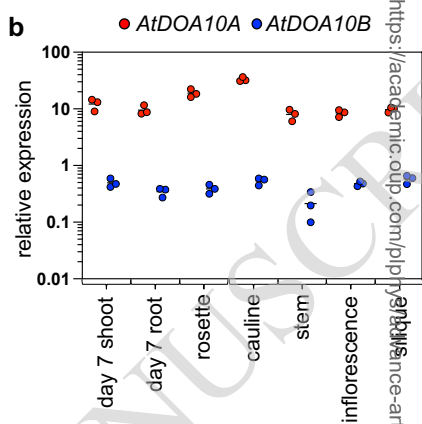
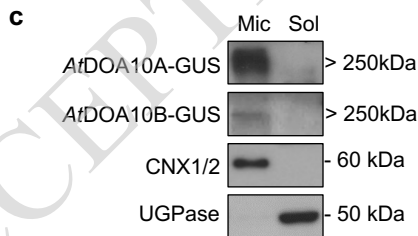
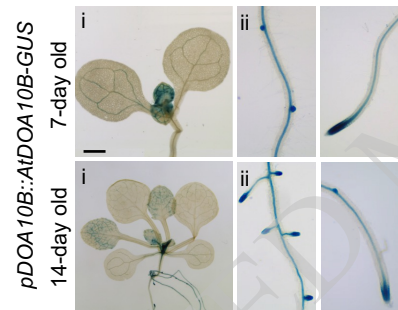
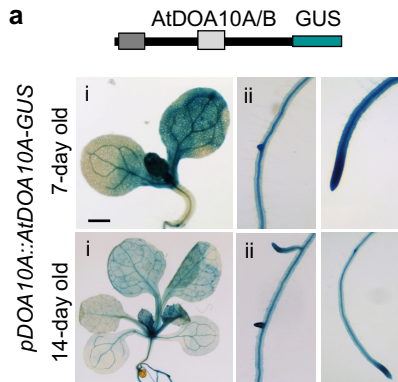
1111 Zhao H, Zhang H, Cui P, Ding F, Wang G, Li R, Jenks MA, Lu S, Xiong L (2014) The Putative E3  
1112 Ubiquitin Ligase ECERIFERUM9 Regulates Abscisic Acid Biosynthesis and Response  
1113 during Seed Germination and Postgermination Growth in Arabidopsis. *Plant Physiol*  
1114 165 (3):1255-1268. doi:10.1104/pp.114.239699

1115  
1116  
1117  
1118

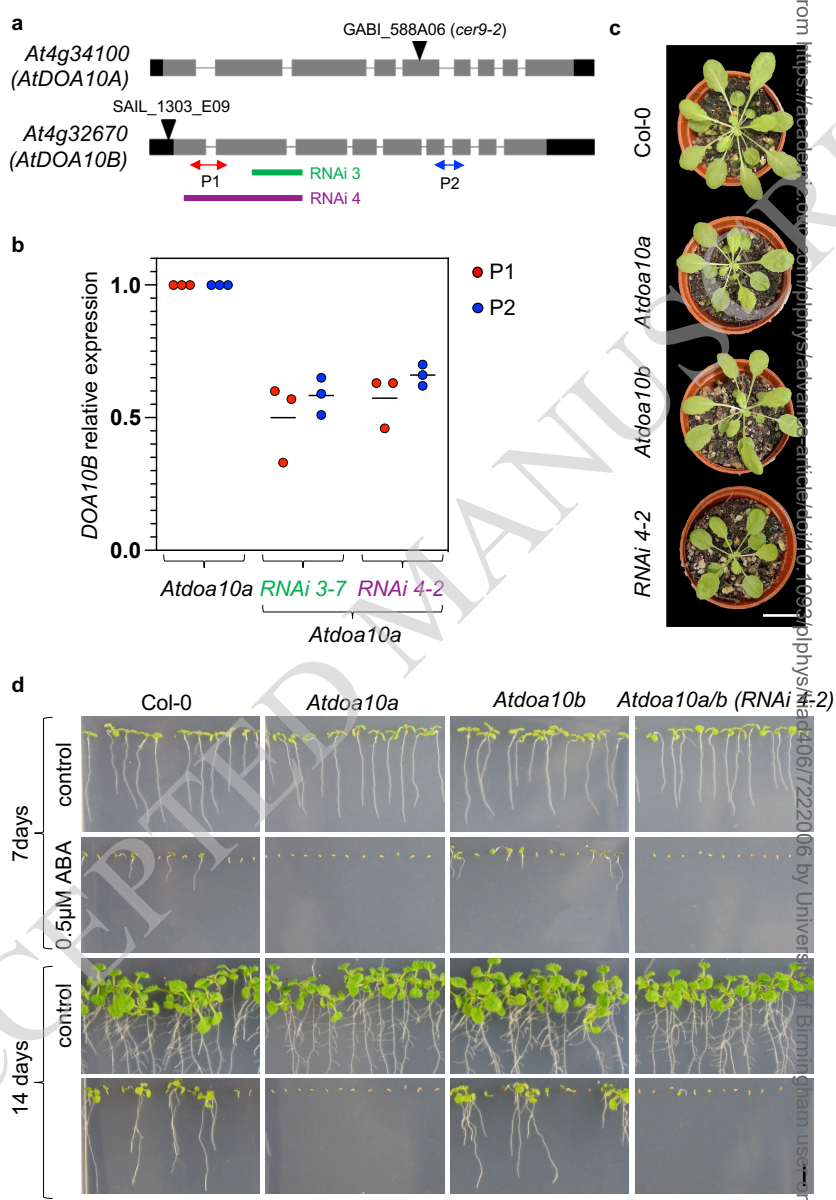
ACCEPTED MANUSCRIPT

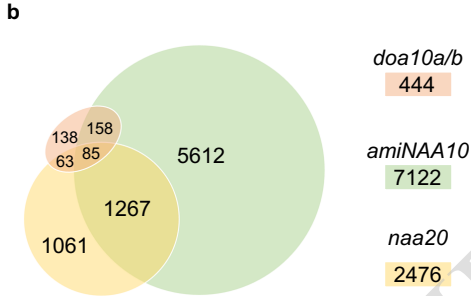
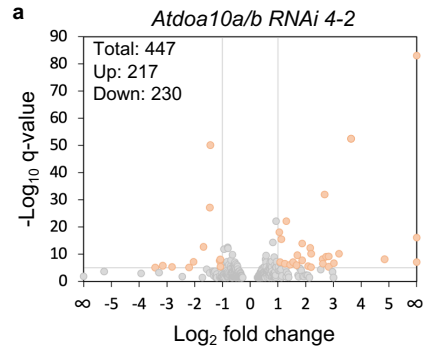






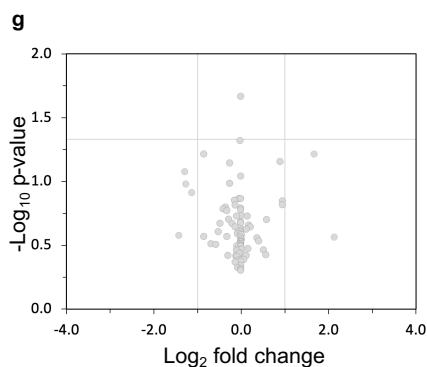
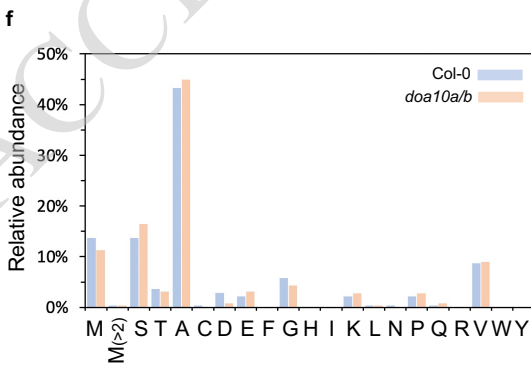
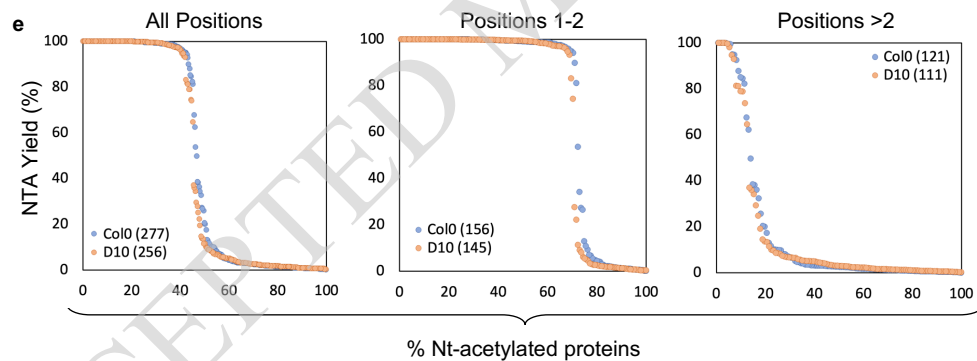
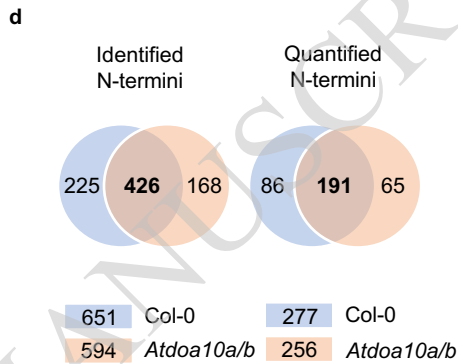
https://academic.oup.com/plip/advance-article/doi/10.1093/plip/phys/kiad047/2222006 by University of Birmingham user on 12 October 2023

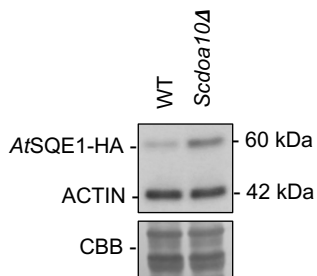
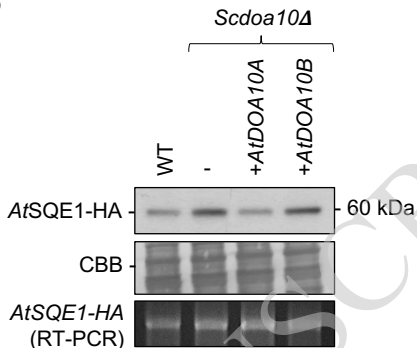
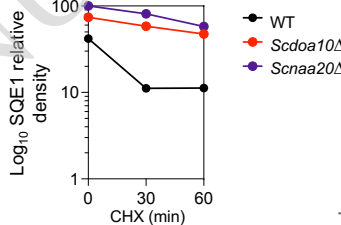
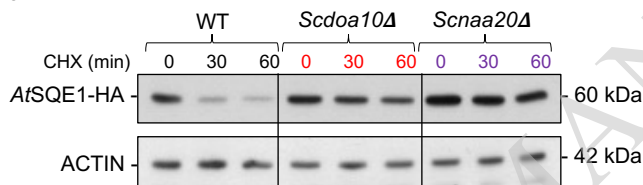
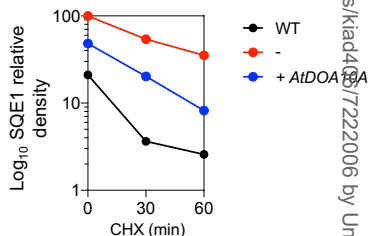
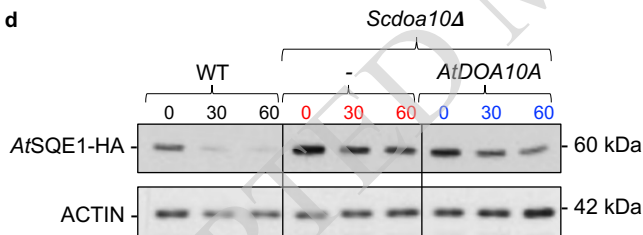
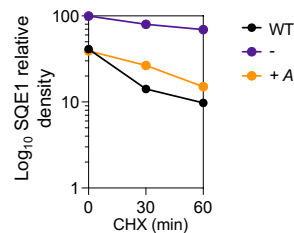
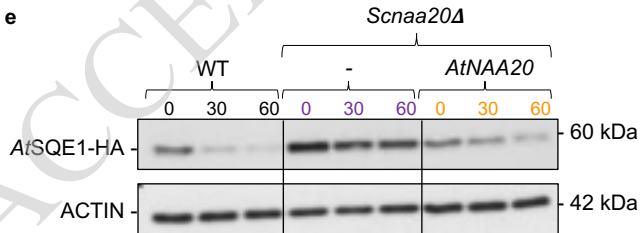




**c**

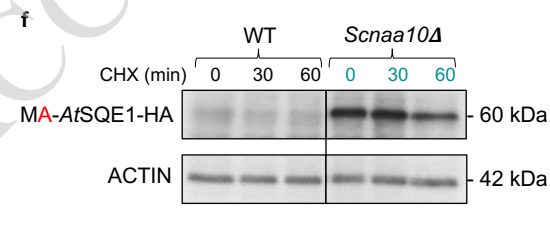
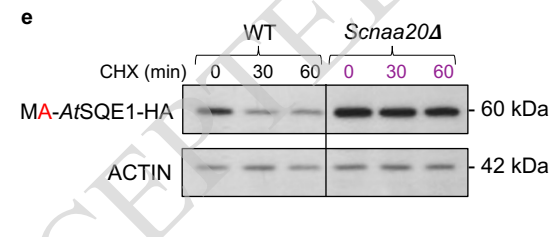
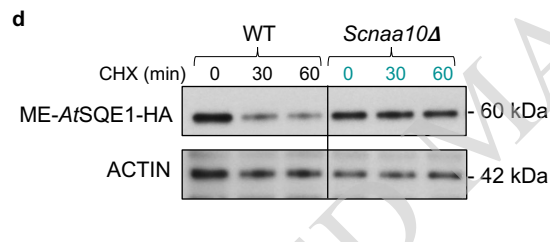
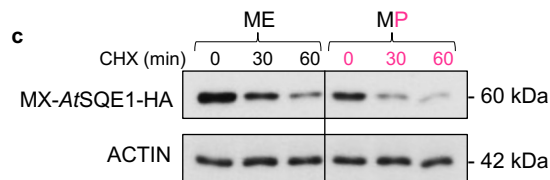
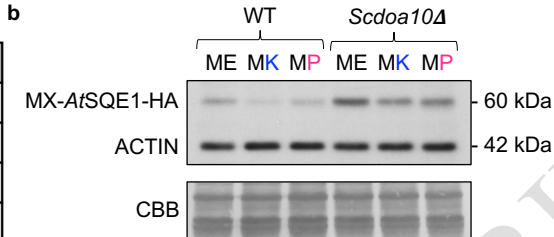
	N-ter peptides	Total	Pos. 1-2	Pos. > 2
Col-0	Identified N-termini	651	337	314
	NTA	311	252	59
	Free	337	85	252
	NTA/Free	3	0	3
Quantitated NTA	NTA > 95%	116	108	8
	5% ≤ NTA ≤ 95%	45	14	31
	NTA < 5%	116	34	82
	Identified N-termini	594	334	260
<i>Atdoa10a/b</i>	NTA	292	252	40
	Free	301	81	220
	NTA/Free	1	1	0
	Quantitated NTA	256	145	111
NTA > 95%	104	98	6	
	5% ≤ NTA ≤ 95%	47	11	36
	NTA < 5%	105	36	69

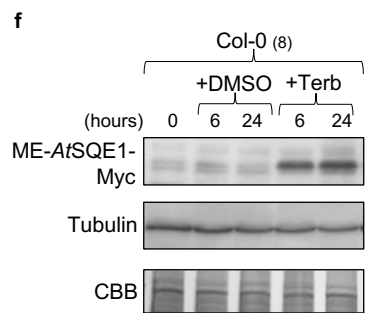
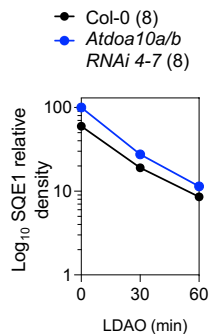
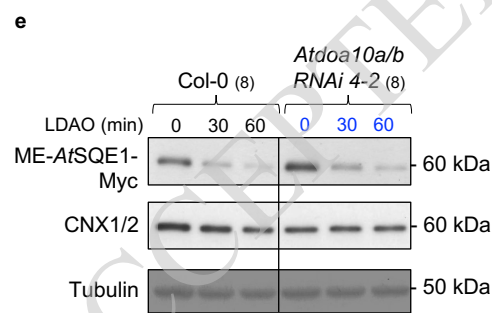
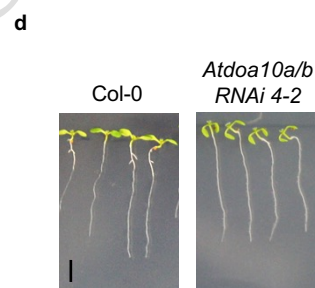
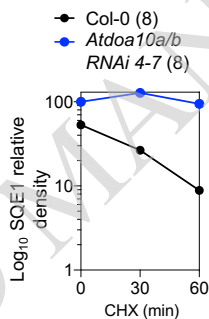
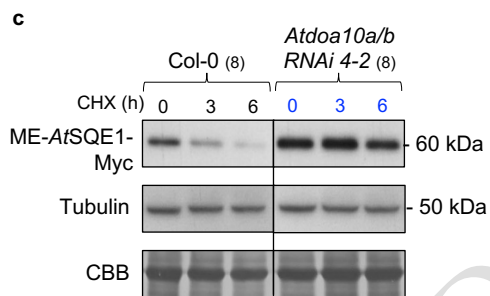
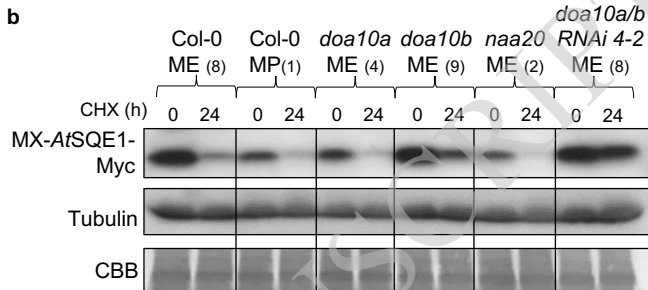
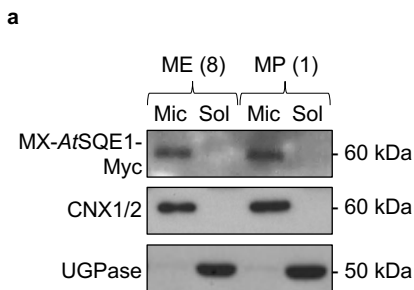


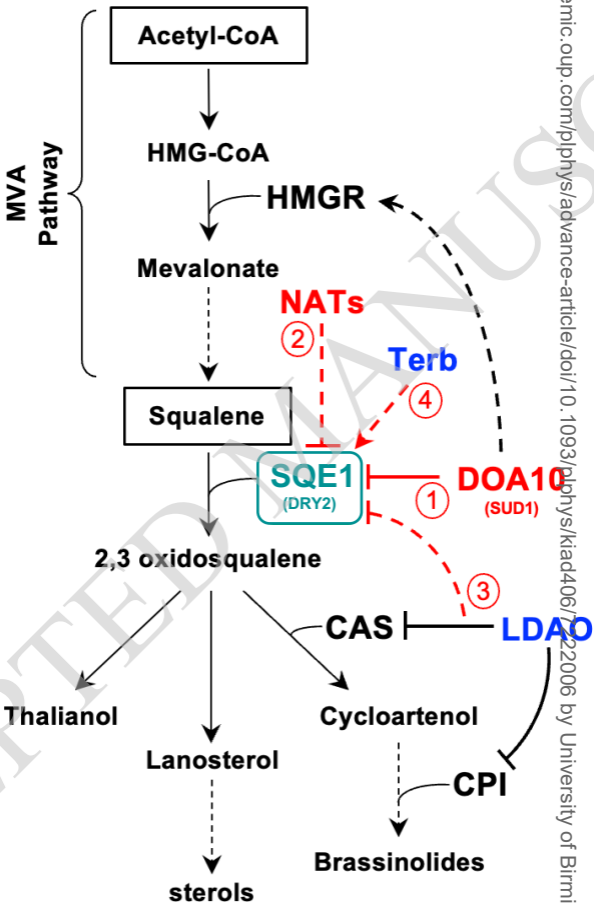
**a****b****c****d****e**

**a**

SQE1-Nt	NAT
<b>ME-</b>	NATB/Naa20
<b>MP-</b>	Not acetylated
<b>MK-</b>	Rarely acetylated
<b>MA-</b>	NATA/Naa10







## Parsed Citations

- Aksnes H, Drazic A, Marie M, Arnesen T (2016) First Things First: Vital Protein Marks by N-Terminal Acetyltransferases. *Trends Biochem Sci* 41 (9):746-760. doi:10.1016/j.tibs.2016.07.005  
Google Scholar: [Author Only](#) [Title Only](#) [Author and Title](#)
- Aksnes H, Goris M, Stromland O, Drazic A, Waheed Q, Reuter N, Arnesen T (2017) Molecular determinants of the N-terminal acetyltransferase Naa60 anchoring to the Golgi membrane. *J Biol Chem* 292 (16):6821-6837. doi:10.1074/jbc.M116.770362  
Google Scholar: [Author Only](#) [Title Only](#) [Author and Title](#)
- Aksnes H, Ree R, Arnesen T (2019) Co-translational, Post-translational, and Non-catalytic Roles of N-Terminal Acetyltransferases. *Mol Cell* 73 (6):1097-1114. doi:10.1016/j.molcel.2019.02.007  
Google Scholar: [Author Only](#) [Title Only](#) [Author and Title](#)
- Aksnes H, Van Damme P, Goris M, Starheim KK, Marie M, Stove SI, Hoel C, Kalvik TV, Hole K, Glomnes N, et al. (2015) An organellar alpha-acetyltransferase, naa60, acetylates cytosolic N termini of transmembrane proteins and maintains Golgi integrity. *Cell Rep* 10 (8):1362-1374. doi:10.1016/j.celrep.2015.01.053  
Google Scholar: [Author Only](#) [Title Only](#) [Author and Title](#)
- Arnesen T, Van Damme P, Polevoda B, Helsens K, Evjenth R, Colaert N, Varhaug JE, Vandekerckhove J, Lillehaug JR, Sherman F, et al. (2009) Proteomics analyses reveal the evolutionary conservation and divergence of N-terminal acetyltransferases from yeast and humans. *Proc Natl Acad Sci U S A* 106 (20):8157-8162. doi:10.1073/pnas.0901931106  
Google Scholar: [Author Only](#) [Title Only](#) [Author and Title](#)
- Ashburner M, Ball CA, Blake JA, Botstein D, Butler H, Cherry JM, Davis AP, Dolinski K, Dwight SS, Eppig JT, et al. (2000) Gene ontology: tool for the unification of biology. The Gene Ontology Consortium. *Nat Genet* 25 (1):25-29. doi:10.1038/75556  
Google Scholar: [Author Only](#) [Title Only](#) [Author and Title](#)
- Bienvenut WW, Brunje A, Boyer JB, Muhlenbeck JS, Bernal G, Lassowskat I, Dian C, Linster E, Dinh TV, Koskela MM, et al. (2020) Dual lysine and N-terminal acetyltransferases reveal the complexity underpinning protein acetylation. *Mol Syst Biol* 16 (7):e9464. doi:10.15252/msb.20209464  
Google Scholar: [Author Only](#) [Title Only](#) [Author and Title](#)
- Bienvenut WW, Giglione C, Meinzel T (2017a) SILProNAQ: A Convenient Approach for Proteome-Wide Analysis of Protein N-Termini and N-Terminal Acetylation Quantitation. *Methods Mol Biol* 1574:17-34. doi:10.1007/978-1-4939-6850-3\_3  
Google Scholar: [Author Only](#) [Title Only](#) [Author and Title](#)
- Bienvenut WW, Scarpelli JP, Dumestier J, Meinzel T, Giglione C (2017b) EnCOUNTER: a parsing tool to uncover the mature N-terminus of organelle-targeted proteins in complex samples. *BMC Bioinformatics* 18 (1):182. doi:10.1186/s12859-017-1595-y  
Google Scholar: [Author Only](#) [Title Only](#) [Author and Title](#)
- Bienvenut WW, Sumpton D, Martinez A, Lilla S, Espagne C, Meinzel T, Giglione C (2012) Comparative large scale characterization of plant versus mammal proteins reveals similar and idiosyncratic N-alpha-acetylation features. *Mol Cell Proteomics* 11 (6):M111015131. doi:10.1074/mcp.M111.015131  
Google Scholar: [Author Only](#) [Title Only](#) [Author and Title](#)
- Buchanan BW, Lloyd ME, Engle SM, Rubenstein EM (2016) Cycloheximide Chase Analysis of Protein Degradation in *Saccharomyces cerevisiae*. *J Vis Exp* (110). doi:10.3791/53975  
Google Scholar: [Author Only](#) [Title Only](#) [Author and Title](#)
- Carland F, Fujioka S, Nelson T (2010) The sterol methyltransferases SMT1, SMT2, and SMT3 influence Arabidopsis development through nonbrassinosteroid products. *Plant Physiol* 153 (2):741-756. doi:10.1104/pp.109.152587  
Google Scholar: [Author Only](#) [Title Only](#) [Author and Title](#)
- Cui F, Liu L, Zhao Q, Zhang Z, Li Q, Lin B, Wu Y, Tang S, Xie Q (2012) Arabidopsis ubiquitin conjugase UBC32 is an ERAD component that functions in brassinosteroid-mediated salt stress tolerance. *Plant Cell* 24 (1):233-244. doi:10.1105/tpc.111.093062  
Google Scholar: [Author Only](#) [Title Only](#) [Author and Title](#)
- Darnet S, Martin LBB, Mercier P, Bracher F, Geoffroy P, Schaller H (2020) Inhibition of Phytosterol Biosynthesis by Azasterols. *Molecules* 25 (5). doi:10.3390/molecules25051111  
Google Scholar: [Author Only](#) [Title Only](#) [Author and Title](#)
- De Vriese K, Pollier J, Goossens A, Beeckman T, Vanneste S (2021) Dissecting cholesterol and phytosterol biosynthesis via mutants and inhibitors. *J Exp Bot* 72 (2):241-253. doi:10.1093/jxb/eraa429  
Google Scholar: [Author Only](#) [Title Only](#) [Author and Title](#)
- Dinh TV, Bienvenut WW, Linster E, Feldman-Salit A, Jung VA, Meinzel T, Hell R, Giglione C, Wirtz M (2015) Molecular identification and functional characterization of the first Nalpha-acetyltransferase in plastids by global acetylome profiling. *Proteomics* 15 (14):2426-2435. doi:10.1002/pmic.201500025  
Google Scholar: [Author Only](#) [Title Only](#) [Author and Title](#)



Doblas VG, Amorim-Silva V, Pose D, Rosado A, Esteban A, Arro M, Azevedo H, Bombarely A, Borsani O, Valpuesta V, et al. (2013) The SUD1 gene encodes a putative E3 ubiquitin ligase and is a positive regulator of 3-hydroxy-3-methylglutaryl coenzyme a reductase activity in Arabidopsis. *Plant Cell* 25 (2):728-743. doi:10.1105/tpc.112.108696

Google Scholar: [Author Only](#) [Title Only](#) [Author and Title](#)

Drazic A, Aksnes H, Marie M, Boczkowska M, Varland S, Timmerman E, Foyn H, Glomnes N, Rebowski G, Impens F, et al. (2018) NAA80 is actin's N-terminal acetyltransferase and regulates cytoskeleton assembly and cell motility. *Proc Natl Acad Sci U S A* 115 (17):4399-4404. doi:10.1073/pnas.1718336115

Google Scholar: [Author Only](#) [Title Only](#) [Author and Title](#)

Foresti O, Ruggiano A, Hannibal-Bach HK, Ejsing CS, Carvalho P (2013) Sterol homeostasis requires regulated degradation of squalene monooxygenase by the ubiquitin ligase Doa10/Teb4. *Elife* 2:e00953. doi:10.7554/eLife.00953

Google Scholar: [Author Only](#) [Title Only](#) [Author and Title](#)

Friedrich UA, Zedan M, Hessling B, Fenzi K, Gillet L, Barry J, Knop M, Kramer G, Bukau B (2021) N(alpha)-terminal acetylation of proteins by NatA and NatB serves distinct physiological roles in *Saccharomyces cerevisiae*. *Cell Rep* 34 (5):108711. doi:10.1016/j.celrep.2021.108711

Google Scholar: [Author Only](#) [Title Only](#) [Author and Title](#)

Gibbs DJ (2015) Emerging Functions for N-Terminal Protein Acetylation in Plants. *Trends Plant Sci* 20 (10):599-601. doi:10.1016/j.tplants.2015.08.008

Google Scholar: [Author Only](#) [Title Only](#) [Author and Title](#)

Gibbs DJ, Bailey M, Etherington RD (2022) A stable start: cotranslational Nt-acetylation promotes proteome stability across kingdoms. *Trends Cell Biol*. doi:10.1016/j.tcb.2022.02.004

Google Scholar: [Author Only](#) [Title Only](#) [Author and Title](#)

Gibbs DJ, Bailey M, Tedds HM, Holdsworth MJ (2016) From start to finish: amino-terminal protein modifications as degradation signals in plants. *New Phytol* 211 (4):1188-1194. doi:10.1111/nph.14105

Google Scholar: [Author Only](#) [Title Only](#) [Author and Title](#)

Gigliione C, Meinert T (2021) Evolution-Driven Versatility of N Terminal Acetylation in Photoautotrophs. *Trends Plant Sci* 26 (4):375-391. doi:10.1016/j.tplants.2020.11.012

Google Scholar: [Author Only](#) [Title Only](#) [Author and Title](#)

Gill S, Stevenson J, Kristiana I, Brown AJ (2011) Cholesterol-dependent degradation of squalene monooxygenase, a control point in cholesterol synthesis beyond HMG-CoA reductase. *Cell Metab* 13 (3):260-273. doi:10.1016/j.cmet.2011.01.015

Google Scholar: [Author Only](#) [Title Only](#) [Author and Title](#)

Goetze S, Qeli E, Mosimann C, Staes A, Gerrits B, Roschitzki B, Mohanty S, Niederer EM, Laczko E, Timmerman E, et al. (2009) Identification and functional characterization of N-terminally acetylated proteins in *Drosophila melanogaster*. *PLoS Biol* 7 (11):e1000236. doi:10.1371/journal.pbio.1000236

Google Scholar: [Author Only](#) [Title Only](#) [Author and Title](#)

Gong X, Huang Y, Liang Y, Yuan Y, Liu Y, Han T, Li S, Gao H, Lv B, Huang X, et al. (2022) OsHYPK-mediated protein N-terminal acetylation coordinates plant development and abiotic stress responses in rice. *Mol Plant* 15 (4):740-754. doi:10.1016/j.molp.2022.03.001

Google Scholar: [Author Only](#) [Title Only](#) [Author and Title](#)

Gouy M, Tannier E, Comte N, Parsons DP (2021) Seaview Version 5: A Multiplatform Software for Multiple Sequence Alignment, Molecular Phylogenetic Analyses, and Tree Reconciliation. *Methods Mol Biol* 2231:241-260. doi:10.1007/978-1-0716-1036-7\_15

Google Scholar: [Author Only](#) [Title Only](#) [Author and Title](#)

Habeck G, Ebner FA, Shimada-Kreft H, Kreft SG (2015) The yeast ERAD-C ubiquitin ligase Doa10 recognizes an intramembrane degron. *J Cell Biol* 209 (2):261-273. doi:10.1083/jcb.201408088

Google Scholar: [Author Only](#) [Title Only](#) [Author and Title](#)

Hershko A, Heller H, Eytan E, Kaklij G, Rose IA (1984) Role of the alpha-amino group of protein in ubiquitin-mediated protein breakdown. *Proc Natl Acad Sci U S A* 81 (22):7021-7025. doi:10.1073/pnas.81.22.7021

Google Scholar: [Author Only](#) [Title Only](#) [Author and Title](#)

Hirsch C, Gauss R, Horn SC, Neuber O, Sommer T (2009) The ubiquitylation machinery of the endoplasmic reticulum. *Nature* 458 (7237):453-460. doi:10.1038/nature07962

Google Scholar: [Author Only](#) [Title Only](#) [Author and Title](#)

Huber M, Armbruster L, Etherington RD, De La Torre C, Hawkesford MJ, Sticht C, Gibbs DJ, Hell R, Wirtz M (2021) Disruption of the N(alpha)-Acetyltransferase NatB Causes Sensitivity to Reductive Stress in *Arabidopsis thaliana*. *Front Plant Sci* 12:799954. doi:10.3389/fpls.2021.799954

Google Scholar: [Author Only](#) [Title Only](#) [Author and Title](#)

Huber M, Bienvenut WW, Linster E, Stephan I, Armbruster L, Sticht C, Layer D, Lapouge K, Meinell T, Sinning I, et al. (2020) NatB-Mediated N-Terminal Acetylation Affects Growth and Biotic Stress Responses. *Plant Physiol* 182 (2):792-806.

doi:10.1104/pp.19.00792

Google Scholar: [Author Only](#) [Title Only](#) [Author and Title](#)

Hwang CS, Shemorry A, Varshavsky A (2010) N-terminal acetylation of cellular proteins creates specific degradation signals. *Science* 327 (5968):973-977. doi:10.1126/science.1183147

Google Scholar: [Author Only](#) [Title Only](#) [Author and Title](#)

Karimi M, Inze D, Depicker A (2002) GATEWAY vectors for Agrobacterium-mediated plant transformation. *Trends Plant Sci* 7 (5):193-195. doi:10.1016/s1360-1385(02)02251-3

Google Scholar: [Author Only](#) [Title Only](#) [Author and Title](#)

Kats I, Khmelinskii A, Kschonsak M, Huber F, Knieß RA, Bartosik A, Knop M (2018) Mapping Degradation Signals and Pathways in a Eukaryotic N-terminome. *Molecular Cell* 70 (3):488-501.e485. doi:10.1016/j.molcel.2018.03.033

Google Scholar: [Author Only](#) [Title Only](#) [Author and Title](#)

Kim HK, Kim RR, Oh JH, Cho H, Varshavsky A, Hwang CS (2014) The N-terminal methionine of cellular proteins as a degradation signal. *Cell* 156 (1-2):158-169. doi:10.1016/j.cell.2013.11.031

Google Scholar: [Author Only](#) [Title Only](#) [Author and Title](#)

Kim JH, Cho SK, Oh TR, Ryu MY, Yang SW, Kim WT (2017) MPSR1 is a cytoplasmic PQC E3 ligase for eliminating emergent misfolded proteins in *Arabidopsis thaliana*. *Proc Natl Acad Sci U S A* 114 (46):E10009-E10017. doi:10.1073/pnas.1713574114

Google Scholar: [Author Only](#) [Title Only](#) [Author and Title](#)

Kong L, Cheng J, Zhu Y, Ding Y, Meng J, Chen Z, Xie Q, Guo Y, Li J, Yang S, et al. (2015) Degradation of the ABA co-receptor ABI1 by PUB12/13 U-box E3 ligases. *Nat Commun* 6:8630. doi:10.1038/ncomms9630

Google Scholar: [Author Only](#) [Title Only](#) [Author and Title](#)

Koskela MM, Brunje A, Ivanauskaite A, Grabsztunowicz M, Lassowskat I, Neumann U, Dinh TV, Sindlinger J, Schwarzer D, Wirtz M, et al. (2018) Chloroplast Acetyltransferase NSI Is Required for State Transitions in *Arabidopsis thaliana*. *Plant Cell* 30 (8):1695-1709. doi:10.1105/tpc.18.00155

Google Scholar: [Author Only](#) [Title Only](#) [Author and Title](#)

Kozak M (1997) Recognition of AUG and alternative initiator codons is augmented by G in position +4 but is not generally affected by the nucleotides in positions +5 and +6. *EMBO J* 16 (9):2482-2492. doi:10.1093/emboj/16.9.2482

Google Scholar: [Author Only](#) [Title Only](#) [Author and Title](#)

Kreft SG, Hochstrasser M (2011) An unusual transmembrane helix in the endoplasmic reticulum ubiquitin ligase Doa10 modulates degradation of its cognate E2 enzyme. *J Biol Chem* 286 (23):20163-20174. doi:10.1074/jbc.M110.196360

Google Scholar: [Author Only](#) [Title Only](#) [Author and Title](#)

Kreft SG, Wang L, Hochstrasser M (2006) Membrane topology of the yeast endoplasmic reticulum-localized ubiquitin ligase Doa10 and comparison with its human ortholog TEB4 (MARCH-V). *J Biol Chem* 281 (8):4646-4653. doi:10.1074/jbc.M512215200

Google Scholar: [Author Only](#) [Title Only](#) [Author and Title](#)

Laranjeira S, Amorim-Silva V, Esteban A, Arro M, Ferrer A, Tavares RM, Botella MA, Rosado A, Azevedo H (2015) *Arabidopsis* Squalene Epoxidase 3 (SQE3) Complements SQE1 and Is Important for Embryo Development and Bulk Squalene Epoxidase Activity. *Mol Plant* 8 (7):1090-1102. doi:10.1016/j.molp.2015.02.007

Google Scholar: [Author Only](#) [Title Only](#) [Author and Title](#)

Leber R, Zenz R, Schrottner K, Fuchsbichler S, Puhlinger B, Turnowsky F (2001) A novel sequence element is involved in the transcriptional regulation of expression of the ERG1 (squalene epoxidase) gene in *Saccharomyces cerevisiae*. *Eur J Biochem* 268 (4):914-924. doi:10.1046/j.1432-1327.2001.01940.x

Google Scholar: [Author Only](#) [Title Only](#) [Author and Title](#)

Li LM, Lu SY, Li RJ (2017) The *Arabidopsis* endoplasmic reticulum associated degradation pathways are involved in the regulation of heat stress response. *Biochem Biophys Res Commun* 487 (2):362-367. doi:10.1016/j.bbrc.2017.04.066

Google Scholar: [Author Only](#) [Title Only](#) [Author and Title](#)

Li Z, Dogra V, Lee KP, Li R, Li M, Li M, Kim C (2020) N-Terminal Acetylation Stabilizes SIGMA FACTOR BINDING PROTEIN1 Involved in Salicylic Acid-Primed Cell Death. *Plant Physiol* 183 (1):358-370. doi:10.1104/pp.19.01417

Google Scholar: [Author Only](#) [Title Only](#) [Author and Title](#)

Linster E, Forero Ruiz FL, Miklankova P, Ruppert T, Mueller J, Armbruster L, Gong X, Serino G, Mann M, Hell R, et al. (2022) Cotranslational N-degron masking by acetylation promotes proteome stability in plants. *Nature Communications* 13 (1):810. doi:10.1038/s41467-022-28414-5

Google Scholar: [Author Only](#) [Title Only](#) [Author and Title](#)

Linster E, Layer D, Bienvenut WW, Dinh TV, Weyer FA, Leenhuis W, Brunje A, Hoffrichter M, Miklankova P, Kopp J, et al. (2020)

**The Arabidopsis N(alpha) -acetyltransferase NAA60 locates to the plasma membrane and is vital for the high salt stress response. *New Phytol* 228 (2):554-569. doi:10.1111/nph.16747**

Google Scholar: [Author Only](#) [Title Only](#) [Author and Title](#)

**Linster E, Stephan I, Bienvenut WW, Maple-Grodem J, Myklebust LM, Huber M, Reichelt M, Sticht C, Moller SG, Meinel T, et al. (2015) Downregulation of N-terminal acetylation triggers ABA-mediated drought responses in Arabidopsis. *Nat Commun* 6:7640. doi:10.1038/ncomms8640**

Google Scholar: [Author Only](#) [Title Only](#) [Author and Title](#)

**Linster E, Wirtz M (2018) N-terminal acetylation: an essential protein modification emerges as an important regulator of stress responses. *J Exp Bot* 69 (19):4555-4568. doi:10.1093/jxb/ery241**

Google Scholar: [Author Only](#) [Title Only](#) [Author and Title](#)

**Liu L, Cui F, Li Q, Yin B, Zhang H, Lin B, Wu Y, Xia R, Tang S, Xie Q (2011) The endoplasmic reticulum-associated degradation is necessary for plant salt tolerance. *Cell Res* 21 (6):957-969. doi:10.1038/cr.2010.181**

Google Scholar: [Author Only](#) [Title Only](#) [Author and Title](#)

**Livak KJ, Schmittgen TD (2001) Analysis of Relative Gene Expression Data Using Real-Time Quantitative PCR and the 2- $\Delta\Delta$ CT Method. *Methods* 25 (4):402-408. doi:https://doi.org/10.1006/meth.2001.1262**

Google Scholar: [Author Only](#) [Title Only](#) [Author and Title](#)

**Lu S, Zhao H, Des Marais DL, Parsons EP, Wen X, Xu X, Bangarusamy DK, Wang G, Rowland O, Juenger T, et al. (2012) Arabidopsis ECERIFERUM9 involvement in cuticle formation and maintenance of plant water status. *Plant Physiol* 159 (3):930-944. doi:10.1104/pp.112.198697**

Google Scholar: [Author Only](#) [Title Only](#) [Author and Title](#)

**Mi H, Muruganujan A, Ebert D, Huang X, Thomas PD (2019) PANTHER version 14: more genomes, a new PANTHER GO-slim and improvements in enrichment analysis tools. *Nucleic Acids Res* 47 (D1):D419-D426. doi:10.1093/nar/gky1038**

Google Scholar: [Author Only](#) [Title Only](#) [Author and Title](#)

**Mueller F, Friese A, Pathe C, da Silva RC, Rodriguez KB, Musacchio A, Bange T (2021) Overlap of NatA and IAP substrates implicates N-terminal acetylation in protein stabilization. *Sci Adv* 7 (3). doi:10.1126/sciadv.abc8590**

Google Scholar: [Author Only](#) [Title Only](#) [Author and Title](#)

**Nakagawa T, Suzuki T, Murata S, Nakamura S, Hino T, Maeo K, Tabata R, Kawai T, Tanaka K, Niwa Y, et al. (2007) Improved Gateway binary vectors: high-performance vectors for creation of fusion constructs in transgenic analysis of plants. *Biosci Biotechnol Biochem* 71 (8):2095-2100. doi:10.1271/bbb.70216**

Google Scholar: [Author Only](#) [Title Only](#) [Author and Title](#)

**Nguyen KT, Lee CS, Mun SH, Truong NT, Park SK, Hwang CS (2019) N-terminal acetylation and the N-end rule pathway control degradation of the lipid droplet protein PLIN2. *J Biol Chem* 294 (1):379-388. doi:10.1074/jbc.RA118.005556**

Google Scholar: [Author Only](#) [Title Only](#) [Author and Title](#)

**Nowosielski M, Hoffmann M, Wyrwicz LS, Stepniak P, Plewczynski DM, Lazniewski M, Ginalski K, Rychlewski L (2011) Detailed mechanism of squalene epoxidase inhibition by terbinafine. *J Chem Inf Model* 51 (2):455-462. doi:10.1021/ci100403b**

Google Scholar: [Author Only](#) [Title Only](#) [Author and Title](#)

**Park SE, Kim JM, Seok OH, Cho H, Wadas B, Kim SY, Varshavsky A, Hwang CS (2015) Control of mammalian G protein signaling by N-terminal acetylation and the N-end rule pathway. *Science* 347 (6227):1249-1252. doi:10.1126/science.aaa3844**

Google Scholar: [Author Only](#) [Title Only](#) [Author and Title](#)

**Rasbery JM, Shan H, LeClair RJ, Norman M, Matsuda SP, Bartel B (2007) Arabidopsis thaliana squalene epoxidase 1 is essential for root and seed development. *J Biol Chem* 282 (23):17002-17013. doi:10.1074/jbc.M611831200**

Google Scholar: [Author Only](#) [Title Only](#) [Author and Title](#)

**Ravid T, Kreft SG, Hochstrasser M (2006) Membrane and soluble substrates of the Doa10 ubiquitin ligase are degraded by distinct pathways. *EMBO J* 25 (3):533-543. doi:10.1038/sj.emboj.7600946**

Google Scholar: [Author Only](#) [Title Only](#) [Author and Title](#)

**Ree R, Varland S, Arnesen T (2018) Spotlight on protein N-terminal acetylation. *Exp Mol Med* 50 (7):1-13. doi:10.1038/s12276-018-0116-z**

Google Scholar: [Author Only](#) [Title Only](#) [Author and Title](#)

**Schmidt CC, Vasic V, Stein A (2020) Doa10 is a membrane protein retrotranslocase in ER-associated protein degradation. *Elife* 9. doi:10.7554/eLife.56945**

Google Scholar: [Author Only](#) [Title Only](#) [Author and Title](#)

**Scott NA, Sharpe LJ, Capell-Hattam IM, Gullo SJ, Luu W, Brown AJ (2020) The cholesterol synthesis enzyme lanosterol 14alpha-demethylase is post-translationally regulated by the E3 ubiquitin ligase MARCH6. *Biochem J* 477 (2):541-555. doi:10.1042/BCJ20190647**

Google Scholar: [Author Only](#) [Title Only](#) [Author and Title](#)

Sharpe LJ, Coates HW, Brown AJ (2020) Post-translational control of the long and winding road to cholesterol. *J Biol Chem* 295 (51):17549-17559. doi:10.1074/jbc.REV120.010723

Google Scholar: [Author Only](#) [Title Only](#) [Author and Title](#)

Shemorry A, Hwang CS, Varshavsky A (2013) Control of protein quality and stoichiometries by N-terminal acetylation and the N-end rule pathway. *Mol Cell* 50 (4):540-551. doi:10.1016/j.molcel.2013.03.018

Google Scholar: [Author Only](#) [Title Only](#) [Author and Title](#)

Starheim KK, Gevaert K, Arnesen T (2012) Protein N-terminal acetyltransferases: when the start matters. *Trends Biochem Sci* 37 (4):152-161. doi:10.1016/j.tibs.2012.02.003

Google Scholar: [Author Only](#) [Title Only](#) [Author and Title](#)

Strasser R (2018) Protein Quality Control in the Endoplasmic Reticulum of Plants. *Annu Rev Plant Biol* 69:147-172. doi:10.1146/annurev-arplant-042817-040331

Google Scholar: [Author Only](#) [Title Only](#) [Author and Title](#)

Swanson R, Locher M, Hochstrasser M (2001) A conserved ubiquitin ligase of the nuclear envelope/endoplasmic reticulum that functions in both ER-associated and Matalpha2 repressor degradation. *Genes Dev* 15 (20):2660-2674. doi:10.1101/gad.933301

Google Scholar: [Author Only](#) [Title Only](#) [Author and Title](#)

Viotti C, Kruger F, Krebs M, Neubert C, Fink F, Lupanga U, Scheuring D, Boutte Y, Frescatada-Rosa M, Wolfenstetter S, et al. (2013) The endoplasmic reticulum is the main membrane source for biogenesis of the lytic vacuole in *Arabidopsis*. *Plant Cell* 25 (9):3434-3449. doi:10.1105/tpc.113.114827

Google Scholar: [Author Only](#) [Title Only](#) [Author and Title](#)

Wiame E, Tahay G, Tyteca D, Vertommen D, Stroobant V, Bommer GT, Van Schaffingen E (2018) NAT6 acetylates the N-terminus of different forms of actin. *FEBS J* 285 (17):3299-3316. doi:10.1111/febs.14605

Google Scholar: [Author Only](#) [Title Only](#) [Author and Title](#)

Xu F, Huang Y, Li L, Gannon P, Linster E, Huber M, Kapos P, Bienvenut W, Polevoda B, Meinel T, et al. (2015) Two N-terminal acetyltransferases antagonistically regulate the stability of a nod-like receptor in *Arabidopsis*. *Plant Cell* 27 (5):1547-1562. doi:10.1105/tpc.15.00173

Google Scholar: [Author Only](#) [Title Only](#) [Author and Title](#)

Zelcer N, Sharpe LJ, Loregger A, Kristiana I, Cook EC, Phan L, Stevenson J, Brown AJ (2014) The E3 ubiquitin ligase MARCH6 degrades squalene monooxygenase and affects 3-hydroxy-3-methyl-glutaryl coenzyme A reductase and the cholesterol synthesis pathway. *Mol Cell Biol* 34 (7):1262-1270. doi:10.1128/MCB.01140-13

Google Scholar: [Author Only](#) [Title Only](#) [Author and Title](#)

Zhang X, Henriques R, Lin SS, Niu QW, Chua NH (2006) *Agrobacterium*-mediated transformation of *Arabidopsis thaliana* using the floral dip method. *Nat Protoc* 1 (2):641-646. doi:10.1038/nprot.2006.97

Google Scholar: [Author Only](#) [Title Only](#) [Author and Title](#)

Zhao H, Zhang H, Cui P, Ding F, Wang G, Li R, Jenks MA, Lu S, Xiong L (2014) The Putative E3 Ubiquitin Ligase ECERIFERUM9 Regulates Abscisic Acid Biosynthesis and Response during Seed Germination and Postgermination Growth in *Arabidopsis*. *Plant Physiol* 165 (3):1255-1268. doi:10.1104/pp.114.239699

Google Scholar: [Author Only](#) [Title Only](#) [Author and Title](#)